Regulation of MMP-13 expression by CD109 in skin cells

by

Melani Kara LIGHTER

Department of Surgery
Division of Experimental Surgery
McGill University, Montreal
Quebec, Canada
July 2011

A thesis submitted to the Faculty of Graduate Studies and Research at McGill University in partial fulfillment of the requirements of the degree of
Master of Science in Experimental Surgery

TABLE OF CONTENTS

ABSTRACT

Our group has identified CD109 as a novel TGF-β co-receptor that inhibits TGF-β signaling in skin cells. To study the role of CD109 in skin *in vivo*, our group has developed transgenic (TG) mice that overexpress CD109 in the epidermis. Previous results have shown that these mice display enhanced wound healing and improved scarring as compared to wild-type (WT) littermates. The aim of this study was to determine the effect of CD109 on the regulation of gene expression in the skin by using a genome microarray. Total RNA isolated from TG and WT mouse keratinocytes was subjected to microarray analysis using Illumina Bead Chip technology. The raw data from the microarray was analyzed using the FlexArray program and 300 genes were found to have differential gene expression in the TG compared to WT keratinocytes; 168 of these genes were up-regulated in the TG keratinocytes and 132 genes down-regulated in the TG keratinocytes. These 300 genes were then analyzed using the Ingenuity program, which implicated them in dermatological diseases and cell interaction. Matrix metalloproteinase-13 (MMP-13) gene expression was found to be up-regulated by 8.4-fold in the TG mouse keratinocytes compared to the WT. MMP-13 is of particular interest due to its ability to breakdown extracellular matrix (ECM) and its important role in wound healing and fibrotic processes. As TIMPs are MMP inhibitors, TIMP-2 was also investigated and found to be up-regulated by 3.03-fold. CXCL1 and αSMA were also studied as they were found to be highly down-regulated in TG compared to the WT mouse keratinocytes. The results obtained from the microarray were confirmed by qRT-PCR and showed an increase at the gene expression level of MMP-13 and TIMP-2 in

the TG keratinocytes and a decrease in the gene expression levels of CXCL1 and αSMA. In order to study MMP-13 further a western blot analysis was performed to look at its protein level. Results showed an increase at the protein level of MMP-13 in the TG keratinocytes although the results were not statistically significant. To investigate MMP-13 *in vivo*, immunohistochemisty was performed and MMP-13 expression was found to be increased in the TG compared to the WT mouse tissue. This study demonstrates increased expression of MMP-13 in TG keratinocytes suggesting that CD109 may modulate wound healing by increasing MMP-13 expression in keratinocytes.

RÉSUMÉ

Notre groupe a identifié un nouveau co-recepteur du TGF-β, CD109, qui inhibe la cascade de signalisation du TGF-β. Pour étudier le rôle de CD109 *in vivo*, nous avons développé des souris transgéniques (TG) qui surexpriment CD109 dans l'épiderme. Les précédents résultats du laboratoire indiquent que les souris TG CD109 cicatrisent mieux que les souris sauvages (WT) de la même portée. Pour déterminer les effets de CD109 au niveau moléculaire, j'ai effectué une étude du génome par puce à ADN. Les ARNs totaux extraits de kératinocytes de souris TG et WT ont été préparés et soumis à une analyse par puce à ADN (Illumina). Les résultats ont été analysés à l'aide des programmes FlexArray et Ingenuity et 300 gènes ont une expression différentielle; 168 de ces gènes ont montré une régulation à la hausse dans les kératinocytes TG et 132 gènes ont montré une régulation à la baisse dans les kératinocytes TG. L'analyse par puce à ADN révèle une forte hausse de MMP-13 (métalloprotéinase matricielle-13) dans les kératinocytes TG, comparée aux keratinocytes WT. Les résultats de cette analyse montrent que, parmi les nombreux gènes surexprimés dans les kératinocytes TG, comparés aux kératinocytes WT, MMP-13 est augmentée de 8,4 fois. MMP-13 est d'un intérêt particulier puisque sa capacité à dégrader la matrice extracellulaire joue un rôle majeur dans les processus de cicatrisation et de fibrose. Comme TIMPs sont des inhibiteurs de MMPs, TIMP-2 a également été étudié et a montré une régulation à la hausse de 3,03 fois. CXCL1 et αSMA ont également été étudiés car ils ont montrés une régulation à la baisse des TG par rapport aux kératinocytes de souris WT. Ces résultats ont été confirmés par qRT-PCR, indiquant que l'expression de l'ARNm de

MMP-13 et TIMP-2 est augmentée dans les kératinocytes TG et une baisse dans les niveaux d'expression des gènes et de CXCL1 αSMA. De plus, afin d'étudier MMP-13, une analyse Western blot a été réalisée pour examiner sa teneur en protéines. Les résultats ont montré une augmentation au niveau des protéines de MMP-13 dans les kératinocytes TG bien que les résultats n'étaient pas statistiquement significatifs. Pour étudier MMP-13 *in vivo*, l'immunohistochimie a été réalisée pour examiner l'expression de MMP-13 et on a trouvé une augmentation dans les TG par rapport au tissu de souris WT. MMP-13 est un important facteur impliqué dans la guérison des plaies cutanées, grâce à sa capacité de dégrader les protéines de la matrice extracellulaire. Cette étude démontre que l'expression de MMP-13 est augmentée dans les keratinocytes TG, suggérant que CD109 pourrait moduler les processus de cicatrisation en induisant une surexpression de MMP-13 dans les kératinocytes.

CONTRIBUTION TO ORIGINAL KNOWLEDGE

1. In order to discover genes regulated by the overexpression of CD109, I used primary keratinocytes isolated from transgenic mice overexpressing CD109 in the epidermis and their wild-type counter parts to perform a microarray analysis using the Illumina bead chip.

2. I analyzed the results from the microarray using the FlexArray and Ingenuity programs. After putting the raw data through a series of statistical tests in FlexArray including Lumi, Cyber-t and FDR, I found 300 genes displayed an increase or decrease in gene expression in the TG keratinocytes compared to their wild-type counter parts. In the Ingenuity program, I found that many of these genes were implicated in dermatological diseases and cell-cell signaling and interaction. MMP-13 gene expression was up-regulated 8.4-fold in the TG keratinocytes compared to the WT ones.

3. I performed qRT-PCR to validate the microarray data. I found that MMP-13 and TIMP-2 gene expression were increased whereas CXCL1 and αSMA gene expression were decreased in the TG keratinocytes compared to the WT which is in agreement with the microarray data. I also performed a western blot to look at the level of protein expression of MMP-13. I found MMP-13 to have a higher protein expression in the TG keratinocytes compared to their WT counter-parts. Immunohistochemistry was performed to look at MMP-13s expression *in vivo.*

MMP-13 expression was found to have a higher expression level in the TG compared to the WT mouse skin.

ACKNOWLEDGMENTS

I would like to thank my supervisor, Dr. Anie Philip for her guidance and support throughout my time in the lab. I would also like to thank everyone in the lab for always being there for me and answering any questions I may have had. A special thanks for Joshua Vorstenbosch who mentored me in the lab.

LIST OF TABLES

LIST OF FIGURES

LIST OF APPENDIX

LIST OF ABBREVIATIONS

ACTA2	Alpha actin 2
Alpha SMA	Alpha smooth muscle actin
AMH	Anti-Müllerian hormone
BMP	Bone morphogenetic proteins
BSA	Bovine serum albumin
CBP	CREB-binding protein
CD109	Cluster of differentiation 109
CXCL-1	Chemokine (C-X-C motif) ligand 1
CXCL-12	Chemokine (C-X-C motif) ligand 12
Cys	Cystein
ECM	Extracellular matrix
EGF	Epidermal growth factor
EMT	Epithilial-mesenchymal transition
ERK	Extracellular-signal-regulated kinases
FDR	False discovery rate
GDF	Growth differentiation factors
Gly	Glycine
GPI	Glycosylphophatidylionositol
Hpx	Hemopexin domain
HRP	Horseradish peroxidase
IgG	Immunoglobulin G
IHC	Immunohistochemistry
IL-24	Interleukin 24
K14	Keratin 14 promoter
kDa	KiloDalton
KGF	Keratinocyte growth factor
KO	Knock out
LAP	Latency associated peptide
LLC	Large latent complex
LL-TGF-β	Large latent transforming growth factor beta
LTBP	Latent transforming growth factor beta binding protein
MAPK	Mitogen-activated protein (MAP) kinases
MH1	MAD homology domain 1
MH2	MAD homology domain 2
MIS	Müllerian inhibitory substance
MMP	Matrix metalloproteinase
MMP-13	Matrix metalloproteinase 13
NaOH	Sodium hydroxide
NES	Nuclear export signal
NF-κB	Nuclear factor kappa-light-chain-enhancer of activated B cells

NLS	Nuclear localization signal
OD	Optical density
p	Phosphorylated
PBS	Phosphate buffered saline
PCA	Principle component analysis
PDGF	Platelet-derived growth factor
PI	Protease inhibitor
PP2C	Protein phosphatase 2C
PPM1	Protein phosphatase 1
RT	Room temperature
RT-PCR	Real time- Polymerase chain reaction
SARA	Smad anchor for receptor activation
Ser	Serine
SLC	Small latent complex
SL-TGF-β	Small latent transforming growth factor beta
SSc	Scleroderma
TBST	Tris-Buffered Saline and Tween
TβRI	Transforming growth factor beta receptor 1
TβRII	Transforming growth factor beta receptor 2
TGF-β	Transforming Growth Factor beta
TG	Transgenic
TIMP	Tissue inhibitor of metalloproteinases
TIMP-2	Tissue inhibitor of metalloproteinases-2
UV	Ultra-violet
WB	Western blot
WT	Wild-type
Zn	Zinc

CHAPTER 1: INTRODUCTION

1.1- TGF-β SUPERFAMILY

1.1.1- TGF-β superfamily members and their functions

Transforming growth factor-β (TGF-β) family members are secreted proteins that activate cellular responses (Shi and Massague 2003). More than 60 TGF-β superfamily members have been identified in multi-cellular organisms and 29 members have been characterized in humans (Feng and Derynck 2005). The superfamily is composed of Bone Morphogenetic Proteins (BMPs)/Growth Differentiation Factors (GDFs), TGF-βs, activins, nodal, lefty and Müllerian inhibitory substance/anti-Müllerian hormone (MIS/AMH) (Gordon and Blobe 2008). The TGF-β family plays a critical role in skin development, homeostasis, wound healing and mediates diverse cellular functions such as proliferation, apoptosis, differentiation and regulation of immune responses (Kane et al 1991, Sellheyer et al 1993, Wang et al 1997). Dysregulation of TGF-β activity has been implicated in many human disorders including cancer, auto-inflammatory diseases (Gordon and Blobe 2008) and skin disorders such as impaired wound healing (Cowin et al 2001, Schmid et al 1993), hypertrophic scarring (Ferguson and O'Kane 2004), psoriasis (Li et al 2004), and malignant melanomas (Hussein 2005, Javelaud et al 2008).

1.1.2- TGF-β subtypes

There are three different TGF-β subtypes in mammals: TGF-β1, TGF-β2 and TGF-β3. Different genes encode these three isoforms but share an amino acid sequence homology of approximately 70% (Shah et al 1995). The amino acid sequence of TGF-β has also been conserved over evolution; this can be seen with human and mouse TGF-β1 differing by only one amino acid (Shull et al 1992). However, these three isoforms have different potencies and biological activities. For example, *in vitro*, TGF-β3 is a more potent inhibitor of DNA synthesis in primary human keratinocytes than TGF-β1 and TGF-β2 (Graycar et al 1989, Shah et al 1995). *In vivo* these differences can be seen in TGF-β null mice. TGF-β1 null mice die within 20 days of birth due to tissue necrosis, inflammation (Shull et al 1992) and vascular defects (Dickson et al 1995). TGF-β2 null mice die in the perinatal period due to cardiac and pulmonary malformations causing insufficiencies (Sanford et al 1997). TGF-β3 null mice die within 24 hours of birth due to poor lung development. These mice also suffer from cleft palates (Proetzel et al 1995).

1.1.3- Synthesis of TGF-β

TGF-β family members are synthesized as homo-dimeric pro-proteins that include a large pro-peptide and a C-terminal mature polypeptide (Annes et al 2003, Gray and Mason 1990). In the Golgi apparatus, furin-like enzymes cleave the pro-peptide, also known as Latency Associated Peptide (LAP), from the TGF-β homodimer. The LAP has a high affinity for mature TGF-β and remains attached to it by a non-covalent bond; this association renders TGF-β inactive (Hyytiainen et al 2004). In the secretory vessels of most cell types, the small latent complex (SLC)

(Saharinen and Keski-Oja 2000)or small latent TGF-β (SL-TGF-β) (Hyytiainen et al 2004) can be covalently bound to an additional protein called the latent TGF-β binding protein (LTBP) which forms another complex termed the large latent complex (LLC) (Saharinen and Keski-Oja 2000) or large latent TGF-β (LL-TGF-β) (Hyytiainen et al 2004). There are four different LTBP isoforms (LTBP-1, -2, -3 and -4) (Koli et al 2004, Olofsson et al 1995). All except for LTBP-4 have been shown to bind all three TGF-β isoforms, while LTBP-4 only binds to TGF-β1 (Saharinen and Keski-Oja 2000). Once secreted, LTBP binds to components of the ECM like heparin and fibronectin, and therefore determines the localization and distribution of TGF-β (Annes et al 2003, Kantola et al 2008).

1.1.4- Activation of latent TGF-β

TGF-β activation is tightly regulated in a spatial, temporal and subtype specific manner. Dissociating from its latent complex activates TGF-β; in this way TGF-βs bioavailability can be controlled (Annes et al 2003, Hyytiainen et al 2004). For example, latent TGF-β can be activated by heat, acid, reactive oxygen species, proteolysis, matrix metalloproteinase (MMPs), thrombospondin binding and integrin-mediated activation (D'Angelo et al 2001, Jenkins 2008). MMP-13 (D'Angelo et al 2001), MMP-2 and MMP-9 (Brooks et al 1996) have been shown to activate TGF-β by using integrin αvβ3 as a docking protein while MMP-14 (or MT1-MMP) (Mu et al 2002) uses integrin αvβ8. Much of the mechanisms of the physiological activation of TGF-β however, still remain unknown (Massague 1998, Murphy-Ullrich and Poczatek 2000).

1.2- ACTIVATION OF TGF-β RECEPTORS AND SIGNAL TRANSDUCTION

1.2.1- Structure of TGF-β receptors

Once TGF-β is active, it propagates its signal through two serine/threonine kinase receptors, TGF-β receptor type I (TβRI) and TGF-β receptor type II (TβRII), which are found on the cell membrane. TβRI contains 503 amino acids and has a molecular weights of approximately 55 kDa while TβRII contains 567 amino acids and a molecular weight of approximately 70 kDa. These receptors consist of an intracellular C-terminal domain with kinase activity, a single transmembrane domain and a short N-terminal extracellular ligand-binding domain (Feng and Derynck 2005, Massague 1998). The TGF-β dimer will bind to a heterotetramer formed by two type I and two type II receptors (Feng and Derynck 2005).

1.2.2- Binding of TGF-β to its receptors

The TGF-β ligand first binds to the TβRII with high affinity (Zhang et al 2009) and induces dimerization of the TβRII (Zhang et al 2009). This TGF-β/TβRII complex recruits TβRI forming a heterotetramer where the constitutively active kinase domain of TβRII comes into close proximity with the GS (Gly-Ser) motif of the TβRI. The transphosphorylation of serine and threonine residues on the GS motif of TβRI by TβRII is required for activation of TGF-β (Souchelnytskyi et al 1996, Wieser et al 1995, Wrana et al 1992, Wrana et al 1994)(Figure 1).

1.2.3-TGF-β superfamily receptor combinations

The downstream effects of TGF-β can be different depending on which TGF-β receptor combination TGF-β binds to. For example, the classic model for receptor combination is TβRII and TβRI (also known as activin receptor-like kinase 5, ALK5) dimerization. It is the L45 loop on TβRI that determines which set of receptor-SMADs (R-SMADs) are recruited. R-SMADs, SMAD2 and SMAD3 will be recruited by the L45 loop of ALK4 and ALK5 but SMAD1/5/8 will be recruited by the L45 loop of ALK1, ALK2, ALK3 and ALK6 (Feng and Derynck 2005). The downstream signal is also cell type specific and can therefore propagate different cellular responses depending on the cell type (Finnson et al 2008, Goumans et al 2002, Goumans et al 2003).

1.3- TGF-β SIGNALING THROUGH THE SMAD (CANONICAL) PATHWAY

1.3.1- Different classes of SMADs and their domains

There are 8 different SMADs in mammalian cells. These SMADs can be grouped into three different categories: 1. R-SMAD (receptor-activated SMAD), which is includes SMAD2, SMAD3 and SMAD1, SMAD5 and SMAD8; 2. Co-SMAD (common-SMAD), SMAD4, which forms a complex with activated R-SMADs and 3. I-SMADs (inhibitory SMADS), SMAD6 and SMAD7, which inhibit TGF-β signaling (Sirard et al 1998, Weinstein et al 1998). R-SMADs and co-SMADs are approximately 500 amino acids in length and have a molecular weight of approximately 50 kDa. The R- and co-SMADs contain two conserved domains, the N-terminal MH1 (MAD-

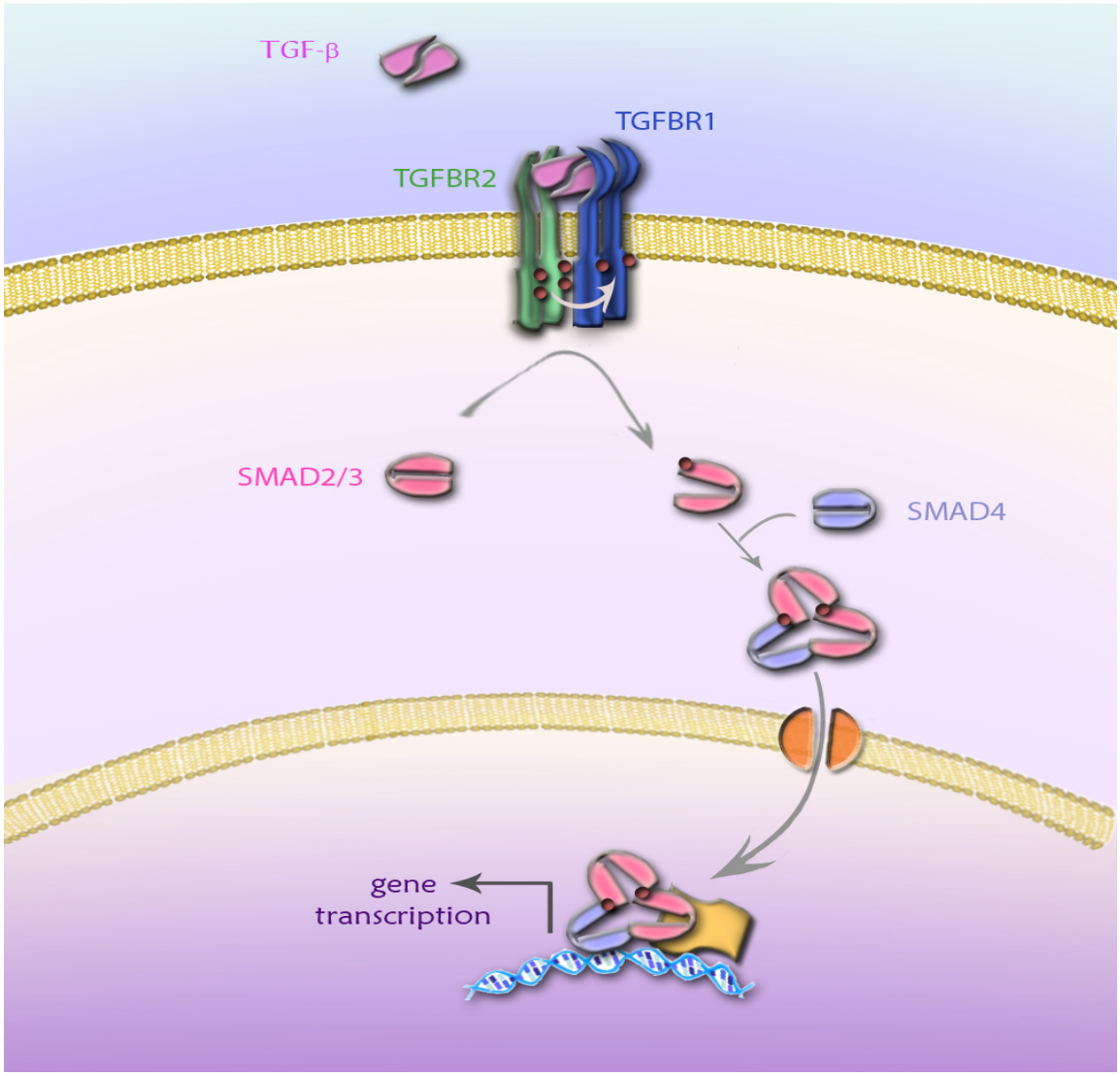

Figure 1: Schematic representation of the TGF-β signaling pathway. TGFβ binds TβRII and TβRI, which leads to the recruitment of R-SMADs to the receptor complex. Upon phosphorylation by the serine/threonine kinase activity of the receptor, R-SMADs can associate with SMAD4 and translocate into the nucleus. Together with transcription factors, the SMAD complex can bind specific gene promoters and either activate or repress transcription of target genes (Schematic diagram created by Albane Bizet).

homology 1) domain and the C-terminal MH2 (MAD-homology 2) domain. R-SMADs contain a characteristic SXS motif at the C-terminus; its phosphorylation drives their activation. The MH2 domain is highly conserved among all the SMADs and possesses a transcriptional activation domain (Massague et al 2005) that is responsible for receptor interaction, homomeric and heteromeric SMAD complex formation and allows direct contact of SMADs to the nuclear pore for nucleocytoplasmic shuttling (Shi and Massague 2003). The MH2 domain of R-SMADs contains a binding site for the activated TβRI, which SMAD4 and I-SMADS lack (Attisano and Lee-Hoeflich 2001, Massague et al 2005). The linker region between the MH1 and MH2 domains contains several phosphorylation sites and allows for cross talk with other pathways. In addition, the linker region of R-SMADs (not SMAD4) contains a PY motif which mediates its interaction with smurfs (SMAD ubiquitination regulatory factor) containing E3 ubiquitin ligases and therefore targets SMADs for degradation. SMADs can also be de-phosphorylated by phosphatases such as PPM1/PP2C (Lin 2007) causing the termination of the TGF-β signal (Shi and Massague 2003).

1.3.2- Activation of R-SMADs

The R-SMADs are the only SMADs that are directly phosphorylated and activated by TβR1 kinases. R-SMADs in contrast to co-SMADs have a more positively charged surface patch on the MH2 domain (Huse et al 2001, Shi and Massague 2003) which is believed to be the binding site of the phosphorylated GS domain of the TβRI. This creates high affinity for binding but not specificity. To create specificity of R-SMAD binding to TβRI, the L45 loop adjacent to the GS domain on TβRI needs to bind to the L3 loop on the R-SMAD (Feng and Derynck 2005, Shi and Massague 2003).

In order for the R-SMADs to be activated, they need to be in close proximity to TβRI. SARA (SMAD anchor for receptor activation) is targeted to early endosomes and is located near the plasma membrane because it contains a phospholipid-binding domain. SARA is able to bind to the SMAD binding domain of SMAD2/3, bringing them close to the plasma membrane. This interaction allows for better recruitment of SMAD2 or SMAD3 to the phosphorylated receptors for phosphorylation (Shi and Massague 2003, Tsukazaki et al 1998).

R-SMADs are directly phosphorylated by activated TβRI. This results in the phosphorylation of two C-terminal serine residues within the flexible SSXS motif. The phosphorylation destabilizes the interaction between SMAD and SARA allowing the dissociation of SMAD2/3 from the complex (Feng and Derynck 2005). The phosphorylation also increases R-SMADs affinity for SMAD4. The C-terminal pSer-X-pSer motif of the R-SMAD and the basic surface pocket of the SMAD4 MH2 domain is important for the formation of the heteromeric complex (Shi and Massague 2003).

1.3.3- Nucleocytoplasmic shuttling of SMADs

In the absence of the TGF-β ligand, R-SMADs are mostly found in the cytoplasm, I-SMADs tend to be in the nucleus while SMAD4 can be found in the nucleus and cytoplasm in equal amounts (Hill 2009). Upon activation of the receptor by TGF-β, the R-SMADs accumulate in the nucleus. It is believed that a portion of the C-terminal, which is conserved among all R-SMADs, acts as a nuclear localization signal (NLS). Importins will recognize the NLS upon R-SMAD phosphorylation and import them into the nucleus. Another proposed method involves the MH2 domain, which binds directly to the nuclear pore complex allowing

SMAD importation and accumulation without importins (Chapnick and Liu 2010, Shi and Massague 2003).

Constant nucleocytoplasmic shuttling is the key event that drives TGF-β signaling. In order to maintain SMAD activity in the nucleus, the receptors remain active for a few hours causing continual shuttling of R-SMADs due to SMAD phosphorylation and de-phosphorylation cycles. The export of SMAD complexes is achieved by the de-phosphorylation of the SSXS motif. This leads to a loss of affinity of R-SMADs to the binding pocket of SMAD4, which results in dissociation of the complex exposing the nuclear export signal (NES) of SMAD4 and subsequently causes nuclear export (Chen et al 2005). Exportin4 exports SMAD2 and SMAD3 (Kurisaki et al 2006).

If the receptors are still activated when the R-SMADs shuttle back into the cytoplasm, they will be re-phosphorylated and return to the nucleus. If the signal has stopped, the SMADs will re-accumulate in the cytoplasm (Hill 2009).

1.3.4- Regulation of gene expression by the SMAD complex

The activation of the TGF-β signaling activity leads to the activation or repressions of different genes (Massague et al 2005). Once the SMAD complex enters the nucleus, it associates with a variety of transcriptional factors such as co-activators or co-repressors, which modulate the amplitude of transcriptional activity. This association depends on cell type and the activation state of other signaling pathways (Feng and Derynck 2005, Massague et al 2005, Shi and Massague 2003).

SMADs interact with co-activators such as CBP/p300, which recruits the RNA polymerase II complex initiating gene transcription (Feng and Derynck 2005). The C-

terminus and MH2 domain of the R-SMADs need to be phosphorylated in order to bind CBP/p300 (Wang et al 2005). SMAD4 helps stabilize the interaction between the R-SMAD and CBP/p300 (de Caestecker et al 2000).

The SMAD complex also interacts with co-repressors like c-Ski/SnoN. They repress gene transcription by recruiting histone deacetylases and mediate the dissociation of the R-SMAD/ SMAD4 complex (Wu et al 2002).

TGF-β signaling is tightly regulated as SMADs modulate a broad range of cellular responses; the balance between the co-activators and co-repressors is therefore imperative.

1.4- TGF-β SIGNALING THROUGH NON-CANOCIAL PATHWAYS

TGF-β can also propagate its signal through SMAD independent pathways by activating other signaling pathways in a cell-type and cell-context specific manners (Feng and Derynck 2005). TGF-β receptor activation can induce Mitogen Activated Protein Kinase (MAPK) pathways, which include the ERK, p38 and JNK pathways (Krishna and Narang 2008). TGF-β also modulates Rho-like GTPases, which contribute to TGF-β induced cell cycle arrest and epithelial-to-mesenchymal transition (EMT) (Ozdamar et al 2005). TGF-β also induces the P13k/AKT pathway (Yi et al 2005). To modulate cytokine production (Guo and Wang 2009), receptor activities (Liu et al 2009) and transcription factors (Verrecchia et al 2001) the TGF-β and other signaling pathways interact through cross-talk. The cross-talk between these different signaling pathways allows for a high degree of regulation and specificity of cellular processes in response to many signals (Guo and Wang 2009).

1.5- NEGATIVE REGULATION OF THE TGF-β SIGNALING PATHWAY

1.4.1- Negative regulation by the inhibitory SMADS

SMAD6 and SMAD7, the inhibitory SMADs, are major regulators of TGF-β signaling because they inhibit signaling using a negative feedback loop (Nagarajan et al 1999, Stopa et al 2000). When the signal is required to be terminated, I-SMADs interact with TβRI via their L3 loop. This does not result in I-SMAD phosphorylation but instead prevents R-SMADs from accessing the receptor and becoming phosphorylated (Hayashi et al 1997, Imamura et al 1997, Nakao et al 1997). Other than competing with R-SMADs for the receptors, SMAD6 has been shown to bind phosphorylated SMAD1 and prevent the formation of the R-SMAD/SMAD4 complex (Hata et al 1998). I-SMADs have also been shown to interfere with R-SMAD transcriptional activity (Zhang et al 2007) and promote de-phosphorylation of TβRI (Shi and Massague 2003). I-SMADs can target the TGF-β receptor to degradation by acting as an adaptor for E3 ubiquitin ligases therefore terminating TGF-β signaling. (Ebisawa et al 2001, Kavsak et al 2000).

1.6- TGF-β CO-RECEPTORS

1.6.1- Betaglycan and Endoglin

TGF-β co-receptors like betaglycan and endoglin (CD105) are cell-surface proteins that bind the TGF-β ligand, thus regulating TGF-β signaling activity (Kirkbride et al 2005).

Betaglycan, the type III receptor, is a cell surface proteoglycan of 853 amino acids (Cheifetz et al 1988, Mythreye and Blobe 2009) with a molecular weight of approximately

200-300 kDa (Lopez-Casillas et al 1993) and is capable of homodimerization (Henis et al 1994). Betaglycan is found in abundance in most cell types but is not expressed in endothelial cells and myoblasts and is therefore more limited in its distribution than TβRI and TβRII (Cheifetz et al 1990, Ohta et al 1987, Segarini et al 1989). Betaglycan binds all three TGF-β isoforms but has the highest affinity for TGF-β2. It facilitates binding of the TGF-β ligand to TβRII, which is most notably seen with the TGF-β2 subtype because TβRII does not bind TGF-β2 on its own (Lopez-Casillas et al 1993, Massague 1998). Depending on cell context, betaglycan can have either positive or negative effects on TGF-β signaling (Lopez-Casillas et al 1994). These positive or negative effects are determined by the size of the cleaved GAG chains of betaglycan (Fukushima et al 1993). If the GAG chains are large they tend to sequester the TGF-β ligand away from the receptors therefore inhibiting signaling while the small GAG chains tend to increase TGF-β signaling (Eickelberg et al 2002).

Endoglin is a 180 kDa TGF-β co-receptor that shares 70% homology with betaglycan. It has a short cytoplasmic domain, a single transmembrane domain and a large extracellular domain that is involved in homodimerization with the TGF-β receptors (Cheifetz et al 1992). Endoglin has a more restricted expression than betaglycan and is expressed in monocytes, endothelial cells and chondrocytes (Massague 1998, Parker et al 2003). Endoglin, unlike betaglycan, cannot bind TGF-β on its own but binds to TGF-β1 and TGF-β3 (not TGF-β2) with high affinity in the presence of TβRII (Letamendia et al 1998). Endoglin has been shown to form a heteromeric complex with betaglycan, which may be important in regulating TGF-β signaling (Wong et al 2000). Endoglin normally acts as a modulator of TGF-βs response by regulating the balance between the TGF-β/ALK5 and the TGF-β/ALK1 pathways. For example, in endothelial cells, endoglins interaction with TGF-β promotes the ALK1/

SMAD1/5/8 pathway and inhibits the ALK5/ SMAD2/3 pathway (Blanco et al 2005, Finnson et al 2010, Lebrin et al 2004). The deletion of endoglin in endothelial cells inhibits TGF-β induced endothelial cell migration and growth (Bobik 2006).

1.6.2- CD109

1.6.2.1- Identification of r150/CD109 as a novel TGF-β co-receptor

Our laboratory has recently identified a novel ~150 kDa TGF-β co-receptor on the cell surface of human keratinocytes. Originally named r150, CD109 displays a high affinity for TGF-β1, but lower affinities for TGF-β2 and TGF-β3. CD109 is also able to form a heteromeric complex with TβRI and TβRII (Tam et al 1998). Further characterization suggests that r150 is a GPI-anchored glycoprotein (Tam et al 2001). CD109 is a member of the α2-macroglobulin family of thioester containing proteins (Haregewoin et al 1994, Sutherland et al 1991, Tam et al 1998). The released soluble form of CD109 binds to TβRI in an isoform specific manner and therefore prevents TGF-β binding to its receptors in human neonatal and in immortalized keratinocytes (HaCaT cells) (Tam et al 2001). These results suggest that CD109 negatively regulates TGF-β signaling (Finnson et al 2006). This indicates that CD109 is a novel TGF-β co-receptor that modulates TGF-β signaling (Figure 2).

1.6.2.2 – Expression of CD109

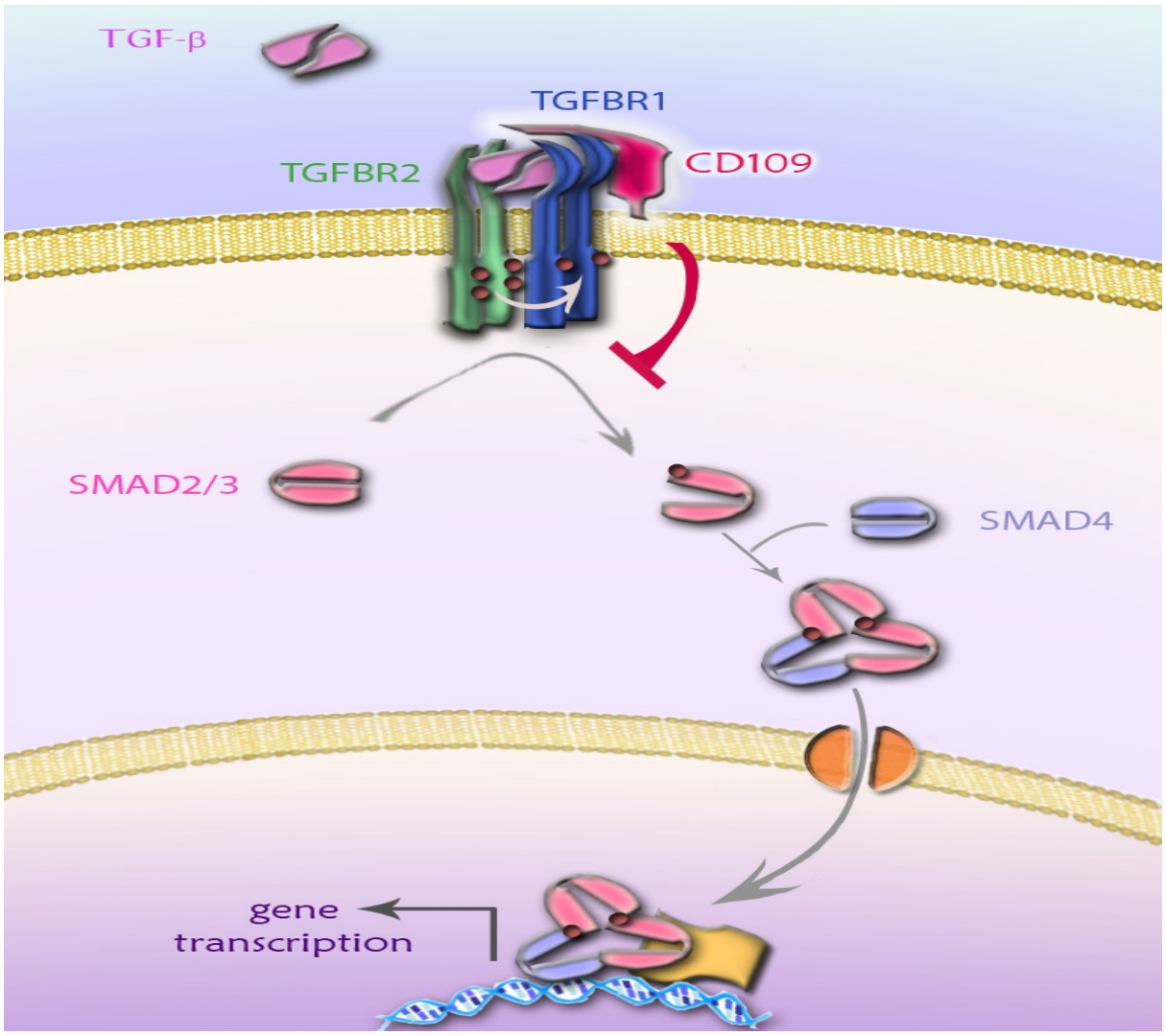

Figure 2: Schematic diagram of CD109 blocking TGF-βs signal transduction. CD109 forms a heteromeric complex with TβRI and TβRII in order to negatively modulate TGF-β signaling.

CD109 is expressed in human keratinocytes (Finnson et al 2006), chondrocytes and mouse and human testis (Hashimoto et al 2004). CD109 expression is up-regulated in many cancers, like basal-like breast carcinoma (Hagiwara et al 2008), glioblastoma, in some adenocarcinomas and sarcomas, while its expression remains low in neuroblastoma, small-cell lung carcinoma, leukemia and lymphoma cell lines (Hashimoto et al 2004). CD109 is also highly expressed in well-differentiated squamous cell carcinomas (SCC), as compared to normal epithelia (Hagiwara et al 2008, Hashimoto et al 2004, Sato et al 2007, Zhang et al 2005). CD109 appears to be mutated in some colorectal cancers (Sjoblom et al 2006). These studies indicate that CD109 may play a critical role during the progression of cancer and other disease (Hagiwara et al 2010).

1.7- ROLE OF TGF-β IN HUMAN SKIN DISEASE AND HOMEOSTASIS

1.7.1- Role of TGF-β in skin development and homeostasis

The skin is composed of layers called stratified epithelium. The outer layer, the epidermis is separated from the inner layer, the dermis, by a basement membrane. During epidermal differentiation, basal keratinocytes stop proliferating and enter suprabasal layers, where they undergo progressive differentiation. As the cells move closer to the surface, they eventually die and fall off the skin (Li et al 2006). TGF-β is a major regulator of skin homeostasis. It plays an important role in the modulation of cell growth, apoptosis, differentiation, ECM production, migration, inflammation and angiogenesis (Massague 2008, White et al 2010). Dysregulation of the TGF-β signaling pathway has been implicated in several skin disorders such as hypertrophic scarring (Armour et al 2007, Seifert and

Mrowietz 2009), psoriasis (Li et al 2004), scleroderma (Leask and Abraham 2004), skin cancer (Li et al 2005) and impaired wound healing (Bennett et al 2003, Cowin et al 2001).

1.7.2- Role of TGF-β during wound healing

Wound healing consists of three phases: inflammation, new tissue formation and remodeling (Gurtner et al 2008, Singer and Clark 1999). During tissue injury, blood vessels are broken and subsequent tissue repair mechanisms such as the coagulation cascade, inflammatory pathways and the immune system are activated. To prevent the loss of blood and fluids, a clot is formed by platelets to re-establish homeostasis and provide a scaffold in the form of a fibrin matrix for chemotaxis to occur (Guo and Dipietro 2010). Neutrophils, macrophages and lymphocytes then infiltrate the wound. Neutrophils clear the invading microbes and cellular debris in the wound area. Two-to-three days post-injury, monocytes appear in the wound bed and differentiate into macrophages. Macrophages in early wound healing release cytokines that promote inflammatory responses by recruiting more leukocytes (Guo and Dipietro 2010).

During the new tissue formation stage which can last 2-10 days after the initial injury, macrophages clear apoptotic cells such as neutrophils, stimulate the growth of keratinocytes and fibroblasts and promote angiogenesis in order to regenerate the tissue (Guo and Dipietro 2010). Keratinocytes first migrate over the injured dermis. In the later part of this stage, fibroblasts are stimulated by macrophages and differentiate into myofibroblasts, which are contractile cells that close the wound. Fibroblasts and myofibroblasts interact to form ECM by producing collagen.

The third stage of wound healing, remodeling, begins 2-3 weeks post injury and can last for over a year. The cells and mechanisms involved in the first two stages cease and most of the endothelial cells, macrophages and myofibroblasts, undergo apoptosis leaving the wound site with collagen and other ECM proteins. Over time the acellular matrix is remodeled with the help of MMPs, which are secreted by fibroblasts, macrophages, endothelial cells and collagen type III. The collagen matrix that is originally laid down is replaced by collagen type I which makes up most of the newly formed tissue. The injured tissue never regains the properties of the uninjured skin (Gurtner et al 2008, Singer and Clark 1999) (Figure 3).

Wound healing involves many cell types, including immune cells, endothelial cells, keratinocytes and fibroblasts. TGF-β plays an important role in wound healing as it is involved in inflammation, angiogenesis, re-epithelialization and connective tissue regeneration, all of which are important processes for proper healing to occur. After injury, TGF-β1 is rapidly up-regulated and secreted by macrophages, platelets and keratinocytes (Singer and Clark 1999). This is important for initiating the inflammatory response, as TGF-β1 acts as a chemoattractant to recruit additional inflammatory cells to the wound site in order to prevent infection (Barrientos et al 2008). In a later stage of wound healing, TGF-β1 induces angiogenesis and enhances migration of keratinocytes and fibroblasts at the wound edge, by up-regulating several MMPs (Lamar et al 2008, Madlener 1998), cell migration associated integrins (Gailit et al 1994) and by promoting the dissolution of cell-cell junctions. Thus, TGF-β1 participates in the re-epithelialization of the wound. Then, TGF-β1 stimulates wound contraction by promoting fibroblasts to differentiate into myofibroblasts

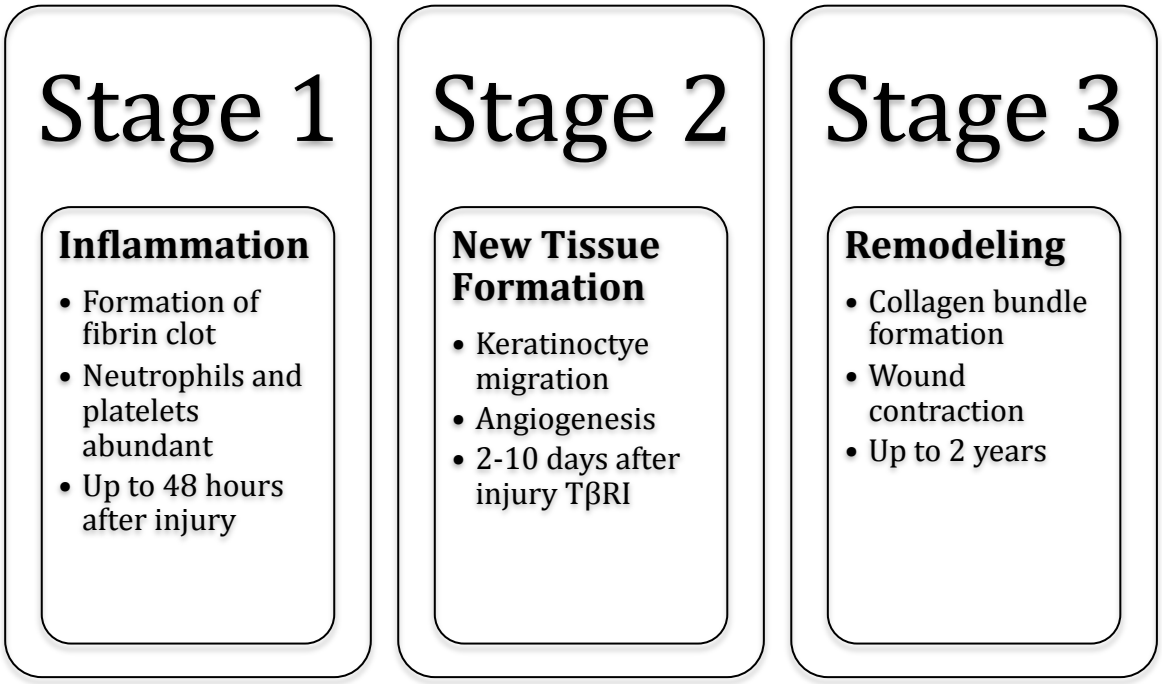

Figure 3: The three classic stages of wound healing. There are three classic stages of would healing. *Stage 1*: Inflammation, the fibrin clot is formed. Neutrophils populate the area to remove bacteria and other foreign particles. *Stage 2*: New tissue formation, keratinocytes migrate across the wound bed for wound closure, new blood vessels are formed. *Stage 3*: Remodeling, disorganized collagen is deposited and wound contraction occurs.

(Desmouliere et al 2005, Montesano and Orci 1988). Importantly, TGF-β is a potent inducer of ECM components, such as collagens and of proteases inhibitors, thereby regulating the remodeling of ECM by fibroblasts (Schiller et al 2004). Although these ECM proteins provide strength and scaffolding to the wound, an overproduction of these proteins causes keloids and hypertrophic scarring (Barrientos et al 2008).

TGF-β1 has dual roles in wound healing. A reduction of TGF-β1 in the wound has been shown to have detrimental effects on the healing of diabetic foot ulcers and chronic venous leg ulcers (Cowin et al 2001, Jude et al 2002, Schmid et al 1993). In order to address this problem, several studies have been conducted using exogenous TGF-β1 in human clinical trials to treat chronic foot ulcers but the promising results from the animal studies did not translate well to humans (Beck et al 1993, Bennett et al 2003, Mulder 2004). On the other hand, an excess of TGF-β1 has been shown to delay cutaneous wound healing in mice that overexpress TGF-β1 in their keratinocytes (Tredget et al 2005, Yang et al 2001). TGF-β1 null mice showed improved wound healing compared to the controls (Koch et al 2000, O'Kane and Ferguson 1997). In order to improve cutaneous wound healing, a balance between TGF-β1s positive and negative effects in wound healing needs to be achieved (Saika et al 2005, Wang et al 1997).

Although TGF-β2 and TGF-β3 are involved in wound healing, unlike TGF-β1, they do not have profound effects. TGF-β2 is involved in all the stages of wound healing as it recruits inflammatory cells to the wound site, promotes angiogenesis and is involved in remodeling by increasing the production of collagen (Barrientos et al 2008, Cordeiro et al 1999). TGF-β3 is important in the inflammatory stage, but has been shown to be an inhibitor of DNA synthesis in human keratinocytes (Tyrone et al 2000) and promotes better collagen

organization in order to reduce scarring, unlike the other two isoforms (Barrientos et al 2008, Shah et al 1995).

1.7.3- Role of TGF-β in skin fibrosis

It has been shown that the expression of TGF-β1 is up-regulated in hypertrophic scars and keloid fibroblasts while TGF-β2s up-regulated expression has been implicated in fibrosis. TGF-β contributes to fibroblast proliferation, their differentiation into myofibroblasts and excessive ECM production and deposition, which is characteristic of fibrosis. Collagen is a downstream target gene of the TGF-β signaling pathway. When its pathway becomes dysregulated during fibrosis, excess disorganized collagen is deposited (Margadant and Sonnenberg 2010, Toriseva and Kahari 2009).

1.8- MMP SUPERFAMILY

1.8.1- MMP superfamily members and their functions

The function of MMPs depends on their capacity to digest a wide range of ECM macromolecules, latent growth factors, cytokines, proteins mediating cell-cell contacts, other pro-proteinases and proteinase inhibitors (Toriseva and Kahari 2009). MMPs also release growth factors from the cell membrane and ECM and activate other MMPs (Gill and Parks 2008).

The activities of most MMPs are very low in normal steady-state tissues but become elevated in various dynamic physiologic situations such as embryonic tissue development and wound healing. The expression of MMPs is transcriptionally controlled by ligand binding

of inflammatory cytokines, growth factors and hormones to their receptors or by alterations in cell-cell and cell-ECM interactions. This MMP expression triggers cellular signals that can activate the MAPK pathway, the SMAD pathway or the NF-κB pathway. The activation and inactivation of certain pathways promote a shift in MMP expression. Their expression is also regulated by the activation of precursor zymogens and inhibited endogenously by tissue inhibitors of metalloproteinases (TIMPs) (Nagase et al 2006, Toriseva and Kahari 2009).

The factors present in cutaneous wound like TGF-β, PDGF, EGF and KGF regulate MMP expression. For example, MMP-1 is induced by the interaction of collagen with migrating wound keratinocytes *in vivo* and is down regulated by KGF *in vitro*. In human fibroblasts, PDGF enhances MMP-1 expression but TGF-β down-regulates its expression. MMP expression can also be regulated by epigenetic modifications such as methylation of chromatin or DNA packing around histones (Toriseva and Kahari 2009).

1.8.2- MMP subtypes

There are 25 MMPs that have been characterized in humans at the amino acid sequence level (Hartenstein et al 2006). Based on domain organization and substrate preference, MMPs are grouped into collagenases, gelatinases, stromelysins, matrilysins, membrane-type (MT-MMP) and other (Table 1). MMPs are mostly secreted proteins but MT-MMPs are linked to the plasma membrane by a transmembrane domain or a GPI anchor (Toriseva and Kahari 2009). The collagenases (MMP-1, MMP-8, MMP-13 and MMP-18) cleave interstitial collagens type I, II and III into fragments but can also digest other ECM molecules and soluble proteins. In mice MMP-1 is functionally substituted for by MMP-13 (Hartenstein et al 2006). The gelatinases (MMP-2 and MMP-9) digest gelatin and other ECM molecules

Enzyme	**MMP**
1. Collagenases	
Collagenase 1 (interstitial)	MMP-1
Collagenase 2 (neutrophil)	MMP-8
Collagenase 3	MMP-13
Collagenase 4	MMP-18 (not found in humans)
2. Gelatinases	
Gelatinase A	MMP-2
Gelatinase B	MMP-9
3. Stromelysins	
Stromelysin 1	MMP-3
Stromelysin 2	MMP-10
Stromelysin 3	MMP-11
4. Matrilysins	
Matrilysin 1	MMP-7
Matrilysin 2	MMP-26
5. Membrane-type MMPs (MT-MMPs)	
i. Transmembrane	
MT1-MMP	MMP-14
MT2-MMP	MMP-15
MT3-MMP	MMP-16
MT5-MMP	MMP-24
ii. GPI-anchored	
MT4-MMP	MMP-17
MT6-MMP	MMP-25
6. Other	
Macrophage elastase	MMP-12/MMP-19
Enamelysin	MMP-20/MMP-21
CA-MMP	MMP-23/MMP-27
Epilysin	MMP-28

Table 1: Matrix Metalloproteinase subtypes. MMPs can be grouped into different subtypes: Collagenases, Gelatinases, Stromelysins, Matrilysins, Membrane-type and other.

such as collagen type IV (basement membrane), V and XI, laminins, elastin and aggrecan core proteins. Stromelysins (MMP-3, MMP-10 and MMP-11) have a similar domain arrangement as collagenases but do not cleave interstitial collagens. They can digest ECM molecules, proteoglycans, glycoproteins and are involved in the activation of proMMPs (Knittel et al 1999, Nagase et al 2006).

1.8.3- Structure of mature MMPs

Most MMPs are extracellular proteins even though MMP-1, MMP-2 and MMP-11 have recently been found intracellularly. Although some MMPs differ slightly in structure, most MMPs have a propeptide of about 80 amino acids, a catalytic metalloproteinase domain of 170 amino acids, a linker peptide, also known as the 'hinge region', and a hemopexin (Hpx) domain of 200 amino acids which mediates molecular interaction and is involved in substrate recognition. All MMPs have a pro-domain and a catalytic domain. The zinc-binding motif is found in the catalytic domain and the 'cysteine switch' motif is found in the propeptide domain. The zinc motif coordinates with the cysteines in the propeptide domain; this Cys-Zn^{2+} coordination keeps proMMPs inactive by preventing catalysis to occur by blocking a water molecule from binding to the zinc atom. The catalytic domain also contains a conserved methionine, which forms a base to support the structure around the catalytic zinc (Nagase et al 2006, Toriseva and Kahari 2009). MMPs domains consist of 5 stranded beta-pleated sheets, three alpha helices and a connective loop. MMPs contains two zinc ions, one, that is catalytic, and one that is structural, and can contain up to three calcium ions that are said to stabilize the structure. The structure of the binding site determines if a peptide substrate can bind to the catalytic domain. The binding pocket, which is near the zinc atom, is

hydrophobic and has variable depths among the MMPs determining its substrate specificity (Nagase et al 2006).

1.8.4- Synthesis and Activation of MMPs

MMPs are synthesized as pre-proenzymes; the signal peptide is removed generating proMMPs during translational processing which is an important regulatory step. Most MMPs are secreted from cells as inactive zymogens or proenzymes. The pro-domain maintains the MMP in latent form because it contains a conserved cysteine residue that interacts with the catalytic zinc ion which is bound to the highly conversed HExxHxxGxxH sequence in the catalytic domain. These proMMPs get activated during proteolytic activation by tissue and plasma proteinases due to the presence of the 'bait' region on the propeptide. First the bait region gets cleaved, leaving an intermediate MMP, which is subsequently processed by the remnants of the pro-domain by the MMP intermediate itself or by other active proteinases, generating the active MMP. MT-MMPs possess a furin-like pro-protein convertase recognition sequence between the pro-and catalytic domains and is therefore more likely to be activated intracellularly within the secretion pathway. The activities of MMPs are regulated by tissue location of the enzyme and endogenous inhibitors (Nagase et al 2006, Toriseva and Kahari 2009).

The hemopexin domain of collagenases is essential for collagenolytic activity. Collagenases unwind the triple helix chains of collagen before cleaving the α chain to break it down. These collagenases contain a collagen groove, which is made up of the catalytic domain and the hemopexin domain. In proMMPs, the groove is narrow and is in its closed

conformation and therefore does not bind collagen. When the MMP is activated, the groove opens up and is able to bind collagen (Nagase et al 2006).

1.9- NEGATIVE REGULATION OF MMPs

1.9.1- Negative regulation by TIMPs

Endogenously, TIMPs are the main MMP inhibitors. TIMPs are 184-194 amino acids in length, have an N-terminal and C-terminal domain and each terminal contains three disulfide bonds (Nagase et al 2006). They are secreted proteins that are soluble in the extracellular space (Toriseva and Kahari 2009). There are four TIMPs, TIMP-1,-2, -3 and -4. TIMPs inhibit MMPs in a 1:1 inhibitor enzyme ratio and it is suggested that all TIMPs can inhibit all MMPs (Nagase et al 2006). The N-terminal domain of the TIMPs interacts with the catalytic site of the active enzyme and the carboxy terminus of the pro-enzyme to inhibit its activity but also prevent its interaction(Gill and Parks 2008, Knittel et al 1999). TIMP-1 poorly inhibits MMP-9 and most MT-MMPs (Toriseva and Kahari 2009), while TIMP-3 null mice exhibit lung abnormalities and faster apoptosis of mammary epithelial cells after weaning. This implicates TIMP-3 as a major regulator of MMPs *in vivo*. In contrast, TIMP-1 and TIMP-2 null mice do not display any obvious abnormalities (Nagase et al 2006).

Although TIMPs are endogenous inhibitors of MMPs, it has been shown that in pathologic states such as fibrosis, MMP and TIMP expression are elevated along side each other (Knittel et al 1999).

1.9.2- Negative regulation by α2-macroglobulin

Another endogenous MMP inhibitor is α2-macroglobulin (Gill and Parks 2008). α2 macroglobulin is a 725 kDa plasma glycoprotein that inhibits proteinases by binding to and sequestering activated MMPs, forming an inactive complex (Grinnell et al 1998) which is cleared by the receptor during endocytosis (Nagase et al 2006). α2-macroglobulin is the inhibitor of MMPs in plasma (Gill and Parks 2008) but can also inhibit MMPs in the ECM (Gill and Parks 2008, Grinnell et al 1998). In burn patients and patients with chronic ulcers, both level of MMP-1 and α2-macroglobulin are increased in plasma (Grinnell et al 1998).

1.10- ROLE OF MMP-13 IN HUMAN SKIN DISEASE AND HOMEOSTASIS

1.10.1- Role of MMP-13 in skin development and homeostasis

The degradation of ECM is an important feature of development, morphogenesis, tissue repair and remodeling (Nagase et al 2006). ECM degradation is essential for normal connective tissue remodeling in embryonic growth and development, morphogenesis, bone growth, resorption and wound healing. In the study done by Hartenstein et al, mice deficient in MMP-13 developed normally and showed no gross phenotypic abnormalities (Hartenstein et al 2006) indicating that MMP-13 is not required for normal development.

1.10.2- Role of MMP-13 during wound healing

During wound healing MMPs have mostly beneficial functions. MMPs are able to drastically alter the activity of their protein substrates. In response to injury, all cells in the environment act to eliminate blood loss, kill foreign particles and close the wound. MMPs participate in the repair process (Gill and Parks 2008).

During inflammation, effector proteins such as metalloproteinases control the production and activity of chemokines and cytokines. MMPs regulate trans-epithelial migration of leukocytes and the compartmentalization of chemokines. Inflammatory cells, epithelial and stromal cells express MMPs in wounded tissues and these MMPs can regulate chemokine activity by direct proteolysis or by promoting the formation of the chemokine gradient. For example, MMP-7 has been shown to be a key regulator of trans-epithelial neutrophil migration following lung injury (Gill and Parks 2008). Chemokines are divided into subfamilies based on their N-terminal cystein residues. The cleavage of CC chemokines by MMPs such as MMP-1 and MMP-3 result in a reduction of chemokine activity by forming receptor antagonists to inhibit downstream signaling. Some CXC chemokines are completely resistant to processing by MMPs while others are readily processed by multiple MMPs. For example, the CXC chemokine, CXCL3 is processed by MMP-1, MMP-2, MMP-8, MMP-9, and MMP-13, which leads to the potentiation of chemokine activities that increase inflammatory cell recruitment. MMP-1, MMP-2, MMP-3, MMP-9, MMP-13 and MMP-14 process CXCL12 resulting in a decrease in chemokine activity and the production of a neurotoxic protein (Gill and Parks 2008). MMPs have a very important role in inflammation as they control chemokine activity, the chemotactic gradient, and the extravasation of leukocytes out of the blood and into injured tissues.

MMPs are involved in growth factor activation such as TGF-β and VEGF. Protienases like MMPs can mobilize TGF-β by releasing it from its matrix bound stores. As mentioned above, TGF-β is secreted as a latent dimeric complex. The LTBP has a strong affinity for several matrix components like fibrillin and is deposited within the ECM. Release of TGF-β/LAP from the ECM requires proteolysis. Active TGF-β can be released from the complex by

proteolysis of MMPs therefore producing mature active TGF-β (Klass et al 2009, Moali and Hulmes 2009, Toriseva and Kahari 2009).

The re-epithelialization phase involves many cellular processes including cell migration, proliferation, differentiation and cell death. During re-epithelialization, MMPs help the cells at the wound margin loosen their cell-cell and cell-ECM contacts so that they can begin to migrate across the wound bed. For example, MMP-1 (collagenase 1) is found in cutaneous wounds during wound healing but not in normal skin. The expression of MMP-1 and many other genes are stimulated by the integrin α2β1 which attaches the dermal matrix rich in type I collagen to the basal lamina. In order for the wound to heal, keratinocytes need to be able to migrate across the wound bed; MMP-1 plays a role in this process by decreasing the affinity of the collagen and integrin interactions. MMP-10 is expressed in epithelium at the migration edge of wounds, implicating its role in cell migration (Gill and Parks 2008).

During resolution and remodeling, MMPs help wound closure by contraction. Mice deficient of MMP-13 have no difference in re-epithelialization but displayed defective wound contraction due to poor formation of αSMA positive myofibroblasts. For the remodeling of collagen to take place the existing collagen needs to be degraded and MMP-13 is capable of cleaving these collagen fibrils (Gill and Parks 2008).

In one study MMP-13 deficient mice showed no alteration in healing of excisional wounds which may be due to enzymatic redundancy (Toriseva and Kahari 2009). In another study MMP-13 KO (knock-out) mice showed a delay in wound closure due to lack of re-epithelialization indicating the importance of MMP-13 in wound closure however, these KO mice did not show a difference in neutrophil infiltration compared to the WT (Hattori et al 2009) which may also be due to enzymatic redundancy.

In the acute stages of hepatic tissue injury, there are high levels of MMPs but low levels of TIMPs, this imbalance results in an overall increased matrix degradation. On the other hand, during chronic hepatic tissue injury MMP levels are low and TIMP levels are high due to the action of TGF-β1 whose role is to promote the expression of TIMPs and to down-regulate the expression of MMPs. This causes an accumulation of ECM and therefore fibrosis (Knittel et al 1999).

MMP-13 is highly expressed in migrating keratinocytes at the leading wound edge during the early phase of the healing process. It is also secreted by dermal fibroblasts in granulation tissue suggesting that it plays an important role in wound healing (Hartenstein et al 2006). Many studies using MMP-13 null mice showed different results with respect to wound healing. This discrepancy may be due to the differences in wound healing pathologies of acute and chronic wound healing (Figure 4).

1.10.3- Role of MMP-13 during skin fibrosis

Fibrosis is a state of increased and altered deposition of newly formed ECM components. It is characterized by an imbalance between enhanced matrix synthesis and diminished matrix breakdown. It has been shown that in liver fibrosis, MMP-2 and TIMP-1 levels are increased resulting in a net inhibition of matrix breakdown and an accumulation of fibrillar collagens (Knittel et al 1999).

Many studies have been conducted to look at the role of MMP-13 during fibrogenesis of the liver, lung and skin. However, all of these studies report different results indicating that there is still a lot to be investigated about MMPs during fibrosis. In the study

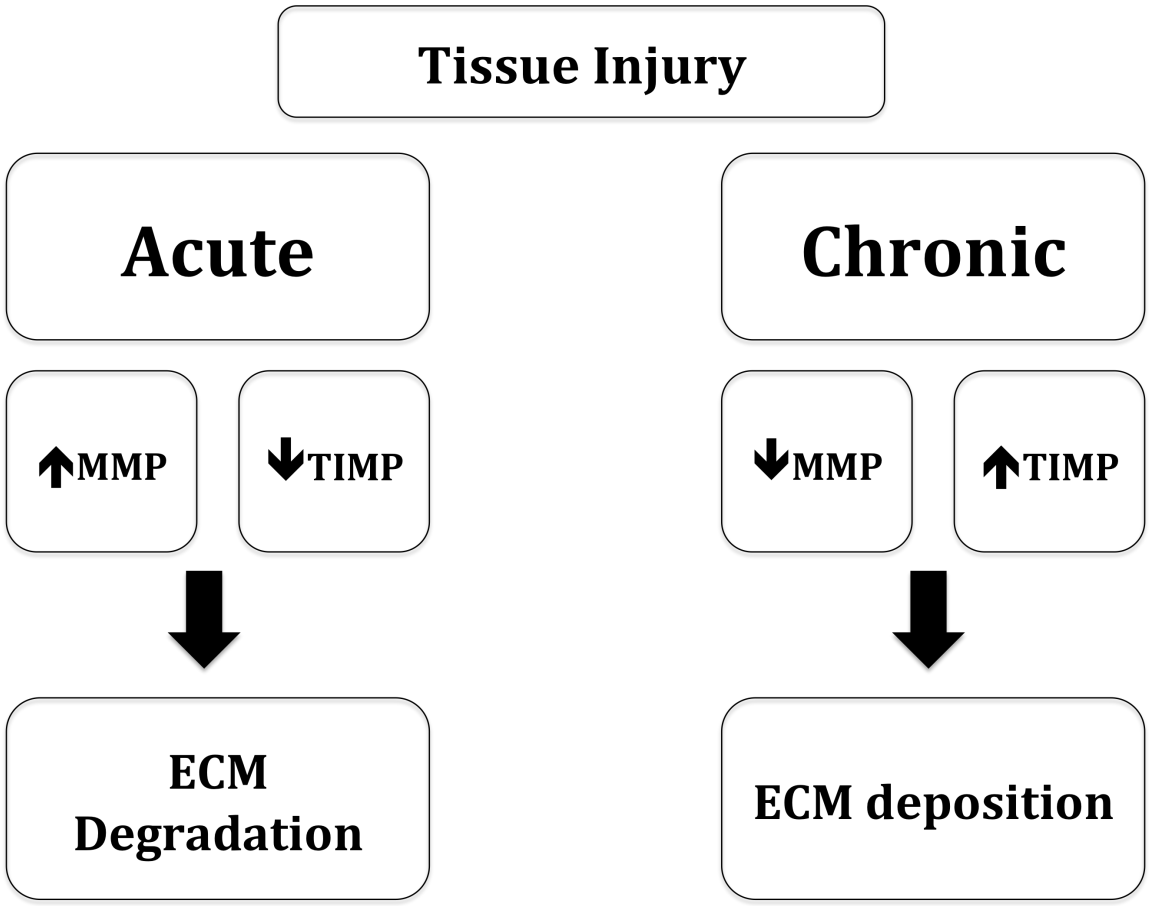

Figure 4: MMP-13 and TIMP-2 during acute and chronic wound healing. MMPs and TIMPs are involved in tissue repair. During acute injury, MMP expression is increased while TIMP expression is decreased so ECM degradation occurs. During chronic injury, MMP expression is decreased while TIMP expression is increased resulting in ECM deposition that can lead to fibrosis.

done by Toriseva et al, they found an elevated expression level of MMP-13 in keloid tissue and certain treatments inducing keloid regression further up-regulated its expression. This elevated expression of MMP-13 by keloid fibroblasts may reflect its attempt to remove the excessive collagen in tissue (Toriseva and Kahari 2009). MMP-13 is also expressed in gingival and fetal skin fibroblasts and responds to TGF-β treatment *in vitro*. MMP-13 expression in chronic wound fibroblasts is increased, but it is still unclear whether increased MMP production contributes to the poor healing of these wounds or if it is induced due to altered stimuli in the wound trying to promote tissue healing (Toriseva and Kahari 2009). On the other hand, scleroderma (SSc) fibroblasts show a marked decrease MMP-13 expression and an increase in TIMP-1 expression in serum. Interestingly, the disease duration was also decreased in these patients (Asano et al 2006).

In the study conducted Flechsig et al, they investigated the role of MMP-13 on radiation-induced pulmonary fibrosis. They found that the WT mice displayed more fibrosis than the MMP-13 KO mice implicating MMP-13 as a potential drug target to attenuate fibrosis. They also showed that inflammatory cell recruitment was increased in the WT mice versus the MMP-13 KO mice alluding to MMP-13s role later in fibrogenesis when the ECM is deposited and during the remodeling phase (Flechsig et al 2010).

1.11- RATIONALE AND OBJECTIVES FOR THE CURRENT STUDY

TGF-β is an important multifunctional growth factor in many cellular processes, including cell growth, ECM production, cell migration, angiogenesis and immune modulation. Dysregulation of its activity has been implicated in several human diseases, notably in skin disorders such as impaired wound healing, hypertrophic scarring and fibrosis. The

therapeutic potential of TGF-β to promote wound healing and TGF-β1 antibodies to reduce scarring are well documented in animal models, but clinical results in humans have been discouraging. This is possibly due to inappropriate timing of administration or unavailability of the delivered factor (O'Kane and Ferguson 1997). A new approach to realize the therapeutic potential of TGF-β in wound healing would be to manipulate the action of endogenous TGF-β locally in the skin using regulatory molecules such as TGF-β co-receptors.

Dr. Philip's laboratory has previously identified a novel TGF-β co-receptor, CD109, in skin cells. CD109 is a GPI-anchored protein that has high affinity for theTGF-β1 subtype and forms a heteromeric complex with the TGF-β signaling receptors. Further studies have shown that CD109 inhibits TGF-β1 signaling in keratinocytes and other cell types *in vitro*, thus decreasing the production of ECM proteins such as type I collagen and fibronectin (Finnson et al 2006, Tam et al 2003). Therefore, CD109 may have a potential therapeutic value in modulating TGF-β action in impaired wound healing states that result in excess ECM protein deposition, such as skin fibrosis, scleroderma and hypertrophic scarring.

Our laboratory has been investigating the effect of overexpression of CD109 using a bleomycin-induced mouse model of skin fibrosis. The mice overexpressing CD109 in the epidermis showed decreased ECM protein deposition, improved collagen architecture and reduced dermal thickness (Al-Ajmi et al 2010). CD109 TG also showed a decreased ECM synthesis, reduced scarring and enhanced healing parameters (Vorsenbosch et al 2010). However, the mechanism by which CD109 may exert its effect on healing and scarring is not well understood. CD109 may regulate the expression of genes important in healing and scarring.

The objective of the study was to identify genes that are differentially expressed in TG mouse keratinocytes overexpressing CD109 compared to their WT counter parts in order to determine how CD109 promotes wound healing.

CHAPTER 2: MATERIALS AND METHODS

2.1- CD109 transgenic mice

Joshua Vorstenbosch, a PhD student in our laboratory, generated CD109 TG mice. Sequenced CD109 cDNA was cloned and inserted into the pGEM-3Z vector (Promega) downstream of a K14-promoter to ensure that CD109 overexpression was restricted to basal keratinocytes in the skin. Detection of the transgene in founder mice was performed by Southern Blot using a probe specific to the transgene that spans the K14-promoter and the CD109 cDNA sequence. To confirm the Southern Blot results, DNA was extracted from mouse-tails by boiling 3mm of tail in 500uL of 100mM NaOH for 30 minutes. The lysate was neutralized with 50uL of 100mM Tris Buffer pH 7, and the resulting DNA was subjected to PCR (polymerase chain reaction) using the same primers used to generate the probe for Southern Blot. Confirmed founder mice were bred at the Transgenic Core Facility (McIntyre Building, McGill University), and mice from each line were sacrificed, the skin was harvested and evaluated for transgene expression by both RT-PCR (to confirm expression of the gene) and Western blot (to evaluate the degree of CD109 protein expression). From the three mouse lines that were created, the line that demonstrated both the presence of the CD109 transgene and the highest expression of CD109 protein in the skin was selected for further breeding at the Transgenic Core Facility. All TG mice and their WT littermates used in this study originated from this single mouse line.

2.2- Isolation Primary Mouse Keratinocytes

TG FVB mice overexpressing CD109 in the skin and WT littermates were used to obtain primary mouse keratinocytes. A litter at only a few days old was sacrificed to obtain cells for primary cell culture. Once sacrificed by decapitation, the carcasses were submersed in proviodine for sterilization. The carcasses were rinsed twice with cold sterile PBS, and submersed in 70% ethanol for 10 minutes and rinsed again twice with cold sterile PBS. The legs and arms were removed and discarded. The tails were cut and put into 1.5ml tubes for genotyping. One carcass at a time was placed on a sterile culture dish where a longitudinal incision was made along the abdomen. The skin was then peeled off of the body and placed dermis side down on a new sterile culture dish. To ensure the skin was as flat as possible on the dish, forceps were used to pull the edges taught. The skin was allowed to dry for 5-10 minutes. Then 5 ml of a 0.25% sterile trypsin (Wisent) solution was added to the culture dish containing the dried skin. Carefully the skin was nudged with forceps to allow it float in the trypsin solution. The dish was incubated at 4°C for 15-24 hours. After incubation, the skin was transferred to a new sterile culture dish where the epidermis was peeled from the dermis using forceps and placed into a new culture dish. The epidermis was minced using scalpels in order to minimize the amount of clumps. 10 ml of growing media was added to the minced epidermis, collected and placed in a T25 flask for growth.

2.3- Genotyping

As mentioned above, in order to identify TG mice, DNA was extracted from mouse-tails by boiling 3mm of tail in 500uL of 100mM NaOH for 30 minutes, with subsequent vortexing at 5-minute intervals. Once dissolved, the lysate was neutralized with 50ul of 1M Tris buffer pH 7. The tubes were centrifuged for 5 minutes at 14 RPMs (revolutions per

minute). The supernatant was collected and placed into new 1.5ml tubes. The resulting DNA was subjected to PCR using the same primers used to generate the probe for Southern Blot. Once the PCR was done, the samples were run on a 2% agarose gel and bands visualized by ethidium bromide staining.

2.4- Cell culture

Once keratinocytes were obtained from TG and WT mice, they were grown in culture. The bottoms of the flasks were pre-treated with collagen to form a collagen matrix that the cells can adhere to. The cells were initially grown in T25 flask until they reached confluency. The keratinocyte media, N-media, was prepared by adding 1 volume of EMEM.06 (450ml of EMEM, 40ml of chelated FBS, 2% penicillin-Streptomycin solution, 0.4% fungizone and 0.0067% of calcium chloride) to 1 volume of CM1 (EMEM.06 conditioned media grown over cultured TG and WT primary mouse fibroblasts, EGF, adinoguanidine nitrate, cholera toxin and hydrocortisone). In T25 flasks the cells were feed 4 ml of TG or WT N-media respectively every 2 days. Once the cells were confluent they were split and plated into T75 flasks. To split the cells, the growth media was aspirated and dPBS for keratinocytes was added twice to wash the cells. Then a 0.25% trypsin solution was added to detach the cells. The cells were incubated for 10 minutes at 37°C. To stop the trypsin reaction, an equal amount of EMEM.06 was added to the flask. The solution containing the trypsin, EMEM.06 and the cells was collected and centrifuged for 10 minutes at 500 Gs (gravitational force). The media was aspirated leaving the pellet behind. The pellet was diluted with N-media and seeded into a new flask.

2.5- RNA Extraction

TG and WT mouse keratinocytes were grown in N-media in T25 flask for RNA extraction. Once confluent, serum free media (SFM) was added to the flasks and placed into the incubator for 4 hours. The SFM was aspirated and the cells washed 2x with sterile dPBS for Kn (keratinocytes). 350 ul of RLT buffer from the RNeasy Mini kit (Qiagen) was added to the flasks. The cells were detached from the bottom of the flask using a cell scraper, collected and placed into a 1.5ml tube provided by the kit. 1 volume of 70% ethanol was added to the tube and up to 700ul of this sample was added to the RNeasy spin column. The RNeasy spin column was centrifuged for 15 seconds at ≥8000 x g (≥10,000 rpm) and the flow through discarded. To eliminate potential genomic DNA contamination, an extra DNase digestion step was taken, as follows. 350ul of RW1 buffer from the kit was added to the column and spun for 15 seconds at ≥8000 x g (≥10,000 rpm) and the flow through discarded. Then 10ul of DNase I stock solution from the RNase-Free DNase set (Qiagen) was added to 70 ul of Buffer RDD. 80ul/sample of the DNase solution was added directly onto the RNeasy spin column membrane and incubated for 15 minutes at room temperature (RT). 350ul of RW1 buffer was added to the spin column and centrifuged for 15 seconds at ≥8000 x g (≥10,000 rpm) and the flow through was discarded. Next, 500 ul of RPE buffer was added and spun for 15 seconds at ≥8000 x g (≥10,000 rpm), the flow through discarded; this step was repeated twice. The spin column was placed into a 1.5ml epindorff provided by the kit. 40 ul of RNase-free water was added directly to the spin column membrane and spun for 1 minute at ≥8000 x g (≥10,000 rpm) to elute the RNA. The RNA was collected and stored at -80°C. This was repeated on 3 Wt and 3 TG mouse kerationcyte flasks.

2.6- RNA quantification

Total RNA was quantified by spectrophotometry. Each RNA sample was diluted 1:20 in DNase, RNase-free water. Samples containing water were used first to take a baseline reading. The OD (260) and OD (280) readings were used to calculate the volume of RNA and water to be added to each tube. All samples were diluted to the same RNA concentration.

2.7- Conversion of RNA into cDNA

The extracted RNA samples were taken out of the -80 ° C freezer and put on ice. First, strip tubes were labeled 'MMLV+' (molony murine leukemia virus) and 'MMLV-'. MMLV+ contains reverse transcriptase, the reaction that converts RNA into cDNA and the MMLV- tubes do not contain reverse transcriptase and are used to confirm that no genomic DNA contamination occurred. For each sample, the known volume of RNA and water was added to the MMLV+ and MMLV– tubes along with 1ul of oligodT (Qiagen) and 1 ul of dNTP mix (100mM, Invitrogen). The MMLV program was run. After stage 1, which was 1 cycle at 65°C for 5 minutes, the program paused to add 4ul of 5x first-strand buffer (Invitrogen) and 2ul of 0.1 M DDT (Invitrogen) to the samples. After stage 2, 1 cycle at 37°C for 2 minutes, the program paused to add MMLV reverse transcriptase to the MMLV + tubes. The program was run to completion. In order to confirm that there was no genomic DNA contamination, a PCR for GAPDH was run on MMLV- samples. The PCR master mix contained 14.5ul of RNase free water (Lonza), 2ul of 10x standard Taq reaction buffer (New England Bio Labs), 0.4 ul of dNTP (Invitrogen), 1ul of the forward GAPDH primer (Invitrogen), 1ul of the reverse GAPDH primer (Invitrogen), 0.1ul of Taq (New England Bio Labs) and 1ul of our corresponding cDNA from the MMLV+ and MMLV- tubes. GAPDH primers have an optimal annealing temperature

of 55°C and the program was run for 30 cycles. Once the program was done, the samples were run on a 2% agarose gel, 150ml of 1x TAE, 3g of agarose and 12ul of ethidium bromide. 2 ul of 10x gel loading buffer (Invitrogen) was added to each sample and loaded into the gel. The ladder used was a 1 kb ladder made from 2-log ladder (New England Bio Labs), 10x gel loading buffer and RNase-free water. The gel was run at 135 V for approximately 30 minutes. The gel was placed into the Dolphin-Doc (Wealtec) where the UV transilluminator detects different levels of GAPDH. Absence of a band in –RT indicated no contamination.

2.8- Primer optimization

The primers were designed using the NCBI website and purchased from Invitrogen. To figure out the best annealing temperature for the primers, a PCR was run using a temperature gradient. The PCR master mix was made, replacing the forward and reserve primers with the ones in question. Then 1ul of cDNA was added to each reaction tube. The samples were run in a temperature gradient from 58°C-62°C. Once the PCR was done, the samples were run on an agarose gel as described above. Under the UV transilluminator, the temperature that showed the strongest signal was selected as the optimal temperature for the primers (Table 2).

2.9- Microarray (Illumina)

The TG and WT primary mouse keratinocytes were incubated with SFM for 4 hours prior to RNA extraction. After RNA was extracted from primary mouse keratinocytes using the RNeasy mini kit, and after quantifying the extracted RNA by using a spectrometer, the RNA sent to Génome Québec for microarray analysis (Illumina). After confirming the

Primer	Forward (5'-3')	Reserve (5'-3')
CD109 (human)	GGCGAATACCATCACAAGTT	TCCTGGGTACGTCCGGTTACA
GAPDH	GGCGTCTTACACCACCATGGAG	AAGTTGTCATGGATGACCTTGGC
MMP-13	AGACTGAGCGCTGCGGTTCAC	CCATGTGGTTCCAGCCACGCAT
TIMP-2	GCCAGCCACCGAGAGGAGGA	CAGCAGCGTGGCTAGCAGCA
CXCL1	ACTCCAACACAGCACCATGA	TACAAACACAGCCTCCCACA
αSMA	GCCAGTCGCTGTCAGGAACCC	CGGCCAGCCAAGTCCAGACG
CXCL12	TTTCGCCTCTAAAGCGCCCAGC	TCCCACGGATGTCAGCCTTCCTC
IL-24	AGCATCCGGCTGTTGAAGCCG	AAGCCTGAGCCAAACAACGGGG

Table 2: Primer nucleotide sequences. This table represents the forward and reverse primer sequences that were used for PCR in this study. All primer sequences are 5' to 3'.

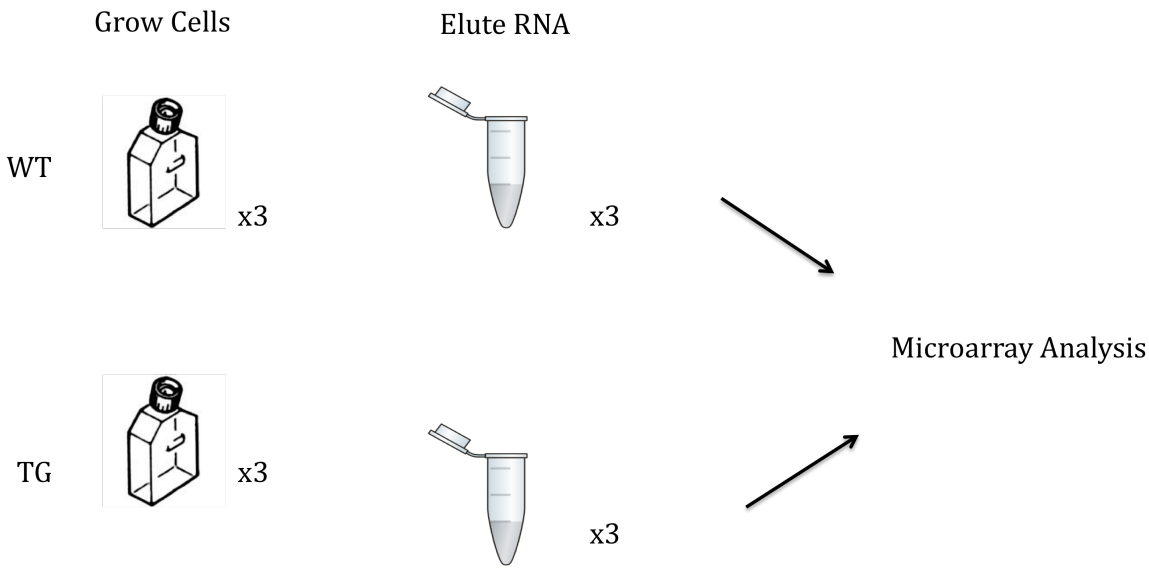

Figure 5: RNA extraction study design. TG and WT primary mouse keratinocytes were obtained and cultured separately. Once confluent, RNA was extracted from the cells using the RNeasy mini kit from Qiagen. The RNA was sent to Génome Québec for microarray analysis (Illumina) (n=3 for each group).

integrity of the RNA and converting it into cDNA, the three samples of TG and WT mouse keratinocyte RNA were subjected to microarray (Illumina) and run on a mouseWG-6_V2 bead chip (Figure 5).

2.10- Microarray Data Analysis

2.10.1- FlexArray

The data was analyzed using FlexArray; a program used for statistical analysis and visualization of microarray expression data, provided by Génome Québec. This program showed the difference in gene expression patterns of the TG and WT keratinocytes. Using the PCA (Principle Component analysis) plot, a variance between the two groups can be seen. The data was put through stringent statistical tests to determine which genes were the most significant in relation to a significant fold change difference and a significant p-value. The raw data underwent Lumi which was designed to pre-process and normalize Illumina microarray data, cyber-T (T-test) that uses a Bayesian estimate of the within treatment variance and the FDR (false discovery rate) which is the expected proportion of true null hypotheses rejected out of the total number of null hypotheses rejected.

2.10.2- Ingenuity

The 300 genes found in FlexArray were put into the Ingenuity program in order to group the genes by signaling pathway, disease and biological functions. This allowed for the analysis of specific genes.

2.11- Semi-quantitative PCR

The cDNA was prepared as mentioned in section 2.7 and the primers were optimized as mentioned in section 2.8. A PCR was run using the PCR master mix mentioned above with cDNA from TG and WT mouse keratinocytes using different primers. The PCR products were analyzed by agarose gel electrophoresis and visualized by UV transilluminator.

2.12- Quantitative RT-PCR

The cDNA was prepared as mentioned in section 2.7, the primers were optimized as mentioned in section 2.8 and a quantitative PCR (qRT-PCR) analysis was performed. Per well, 10ul of iQ™ SYBR®Green (Bio-Rad), 7ul of RNase free water, 1 ul of the forward primer, 1 ul of the reverse primer and 1ul of cDNA was added to make the qRT-PCR mix. Each sample was run in duplicate in order to eliminate pipetting errors. At the bottom right of each plate, two wells were designated for GAPDH using GAPDH primers and the same cDNA each time for inter-run calibration. The program Bio-Rad CFX Manager was used to run the qRT-PCR. In this case, stage 1 was run at 95°C for 3 minutes, stage 2 at 95°C for 15 seconds, the temperature at stage 3 varied depending on the primers optimal annealing temperature and stage 4 at 72°C for 30 seconds. This cycle was repeated 39 more times. At the end, each sample was analyzed for a melt curve with temperatures between 65°C and 95°C. MMP-13, TIMP-2, CXCL1 and αSMA were run. An identical plate with GAPDH was also run in order to normalize the samples to a baseline. Once the program was done, the melt curve was analyzed. In this case the melt curve was above the threshold and had only one peak.

2.13- Western Blot

TG and WT keratinocytes were starved for 4 hours in SFM; 1 ml of the conditioned media was collected and placed into 1.5ml siliconized tubes with 10ul of protease inhibitor (PI). A protein assay was performed on the samples in order to equalize the protein concentration in each sample for loading. The samples and a selection of BSA protein standards (10 μg/μL, 5 μg/μL, 2.5 μg/μL, 1.25 μg/μL, 0.625 μg/μL, and 0.3125 μg/μL) were assayed using D/C Protein Assay Kit (BioRad). The reaction was read by a spectrophotometer at 655 nm on a Bio-Rad Microplate Reader (Bio-Rad, Mississauga, ON). The protein concentration within samples was determined by extrapolating from a standard curve plotting known BSA protein concentrations against OD_{655} readings. Protein-rich supernatant samples were normalized to a concentration of 1 μg/μL using SFM and 5X electrophoresis reducing sample buffer (20% volume) to ensure equal loading of the samples into the gel. The samples were boiled for 10 minutes at 100°C, allowed to cool for 10 minutes and loaded into an SDS-PAGE gel (10%) and run at 100V. The protein was transferred to a nitrocellulose membrane (Whatman) using a transfer apparatus. Once the transfer was done, Ponceau Red (Sigma-Aldrich) was placed on the membrane to verify effective transfer of the protein. A picture was taken of the membrane containing the ponceau and was used as a loading control. Once the Ponceau was washed off, non-specific sites were blocked in 5% milk in TBST (Tris-buffer saline, 1% Tween) for 1 hour at RT on a shaker. The primary antibody was added, MMP-13 (Abbiotec) at a concentration of 1:500 in 5% milk in TBST overnight at 4°C. The next day the primary antibody was removed and the membrane was washed in TBST and the secondary antibody, anti-Rabbit IgG HRP-linked antibody (Cell Signaling) at a concentration of 1:1500 in 5% milk in TBST was placed on the membrane for

1 hour at RT on the shaker. The membrane was subjected to chemo luminescence analysis (ECL, Vector) and developed on photographic film (Denvile).

2.14- Immunohistochemisty

Slides containing normal TG and WT mouse skin were prepared. Histological sections were de-paraffinized in xylene (3 changes, 10 minutes each) and rehydrated in decreasing concentrations of ethanol (100%, 95%, 70%). Following a brief wash in distilled water (2 changes, 5 minutes each), the slides were placed in a glass slide holder and heated in 10X citrate buffer in the microwave for 10 minutes (power level 30) for antigen retrieval. The slides were allowed to cool for 30 minutes, washed in distilled in water (3 changes, 5 minutes each), and incubated at RT in 3% hydrogen peroxide for 10 minutes on the shaker. The sections were subsequently washed in distilled water (2 changes, 5 minutes each), followed by TBST (5 minutes) and blocked with 5% normal goat serum (NGS) solution in TBST (35 μL per tissue section, a hydrophobic pen was used to encircle tissue sections on the slide). Next, slides were washed in TBST (5 minutes) and anti-MMP-13 antibody (Abbiotec, raised in rabbit) diluted to a concentration of 1:200 in 5% normal goat serum in TBST was applied to sections and left overnight at 4 °C. To serve as a negative control, the primary antibody was not added to one tissue sample per slide.

Following incubation with the primary antibody, the slides were washed in TBST (3 changes, 5 minutes each). A secondary biotinylated antibody (rabbit) was applied at 1:500 in TBST and slides were left to incubate for 30 minutes at RT followed by a subsequent wash in TBST (3 changes, 5 minutes each). ABC reagent (5% in TBST) was applied to all sections for 30 minutes followed by a wash in TBST (3 changes, 5 minutes each). To initiate the reaction

with MMP-13, DAB was added to each tissue specimen on the slides, and slides were observed under the microscope. Once stained, the slides were placed in distilled water to stop the reaction. Finally, the slides were counterstained in Harris' Hematoxylin for 30 seconds, washed in distilled water for 1 minutes, dehydrated in increasing concentrations of ethanol (95%, 100%, 10 seconds, 2 changes each), and cleared in xylene (2 changes, 10 seconds each). In order to protect the tissue, slides were mounted with Permount, a resinous mounting medium and allowed to dry before being observed. The sections were photographed under the microscope.

2.15- Statistics

Numerical results were represented as means of n independent experiments ± SEM, according to the recommendations found in Cumming et al 2007. A two-tailed Student t test was used to determine statistical significance between two groups. A value of $p<0.05$ was considered significant.

CHATER 3: RESULTS

3.1 Generation of CD109 transgenic mice

CD109 TG mice were generated by Joshua Vorstenbosch, a PhD student in our laboratory. The previously sequenced CD109 cDNA was cloned and inserted into a vector downstream of a K14-promoter that restricted the overexpression of the transgene to basal keratinocytes (Figure 6a). The mice from the TG and the WT line were sacrificed and the skin was harvested and evaluated for transgene expression by both RT-PCR (to confirm expression of the gene) and Western blot (to evaluate the degree of CD109 protein expression) (Figure 6b). From the three mouse lines available, the line that demonstrated both the presence of the CD109 transgene and the highest expression of CD109 protein in the skin was selected for further breeding.

3.2 Genotyping mice

For *in vitro* studies, in order to determine if the primary mouse keratinocytes to be harvested were TG or WT, a 3 mm portion of a newborn mouse-tail was cut during the tissue harvesting procedure. For *in vivo* studies, the mice were raised to maturity, and a small portion (3 mm) of the tail was cut from each mouse for genotyping. The 3 mm pieces of the mouse-tails were used for DNA extraction. Using a primer specific to the transgene that spanned the K14-promoter (forward Intron F) and the CD109 (reverse CD109) cDNA sequence, a PCR was run to amplify DNA from the mouse-tails in order to determine which mice were TG and which were WT. Once genotyped, for the *in vitro* studies, the primary mouse keratinocytes were placed in their respective flasks for culture and the mice for

a.

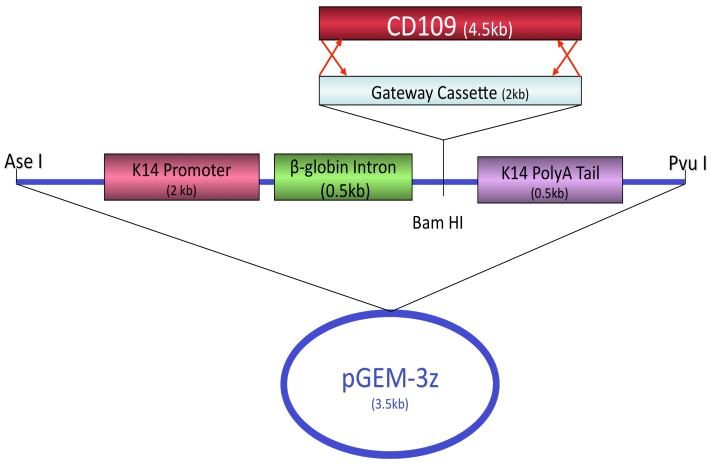

b.

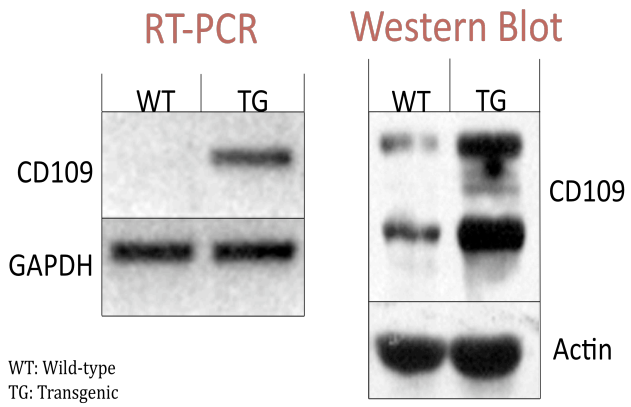

Figure 6: (a) CD109 transgene vector; (b) CD109 transgene expression by RT-PCR and Western blot. a. CD109 cDNA was cloned and inserted into a pGEM-3Z downstream of a K14 promoter, which spatially restricts overexpression of the transgene to basal keratinocytes in the skin. b. RT-PCR of founder mouse used for transgenic line confirming expression of the CD109 transgene; GAPDH was used as a loading control. Western blot of the same TG mouse confirming overexpression of CD109 protein in skin homogenates in comparison to WT control littermate; actin used as a loading control (completed by Joshua Vorstenbosch).

in vivo studies were labeled using the ear punch system in order to keep track of which mice from each litter belonged to which genotype (Figure 7).

3.3- Microarray Data

The TG mice described above have been used for many different studies in our laboratory including wound-healing studies that looked at scarring parameters, collagen and fibronectin synthesis as well as the rate of wound closure. Our group has been focusing on how the overexpresstion of CD109 in the TG mice affects TGF-β downstream signaling. In order to study how the overexpression of CD109 effects gene transcription in TG mouse keratinocytes compared to their WT counterparts, a genome wide microarray was performed using a mouseWG-6_V2 bead chip.

3.4- Microarray Analysis

3.4.1- FlexArray

The data from the microarray was analyzed initially using the FlexArray program provided by Génome Québec, which is a Microsoft Windows software package for statistical analysis and visualization of microarray expression data. The raw data obtained from the microarray analysis is displayed by probe number and shows the fold change of mRNA expression levels and the p-values of each gene. There were over 30,000 genes to be analyzed. The first step was to import the annotations in order to determine which probe ID corresponded to which gene. The annotations can be found on Illumina.com and imported

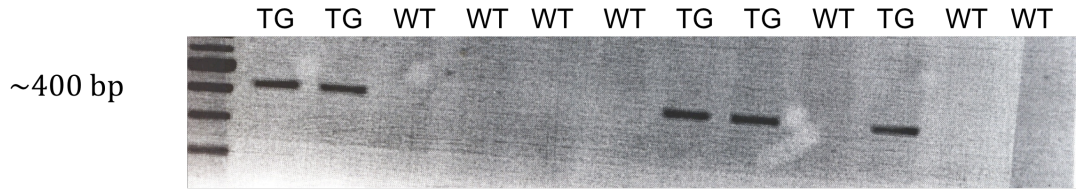

Figure 7: Mouse Genotyping by PCR. Using a primer specific to the CD109 transgene that spanned the K14-promoter and the CD109 cDNA sequence, DNA from mouse tails was run on an agarose gel. The CD109 band is detected ~400 bp (basepairs).

into FlexArray; in this case the mouseWG-6_V2 Illumina bead chip annotation file was used. These genes underwent rigorous statistical testing in order to determine which ones were differentially expressed in the TG and WT mouse keratinocytes. Statistical tests like Cyber-T, which is used to determine the probability that these results were obtained by chance and FDR, which performs multiple hypothesis testing and raises the minimum p-value in order to obtain better results were used. I first looked at the PCA plot, which reduces the multi-dimensional data set; this tool is used for quality control. From the PCA plot a clear division can be seen between the TG and WT groups, with a variance of 75.513% (Figure 8). The PCA plot was not used to accept or reject the data but was used to see if variance existed between the two experimental groups. To run an algorithm, group 2 (TG) was subtracted from group 1 (WT). After the statistical tests, a volcano plot was obtained which excluded all genes that either had a fold change between -2 and +2 (x- axis) when comparing the TG and WT groups and a p-value higher than 0.05 (y-axis) (Figure 9). From this volcano plot, 300 genes were found to be either significantly over- or under-expressed in the TG compared to the WT mouse keratinocytes. The first gene explored was CD109, as it is overexpressed in the TG mice, it was shown to be overexpressed with a fold change increase of 2.169 in the TG keratinocytes compared to their WT counter-parts (Figure 10). The other 300 genes were looked at more carefully in order to determine which ones would be of interest to the group.

3.4.2- Ingenuity

In order to determine relevant pathways and related diseases linking these genes together, the 300 genes identified in FlexArray were put into the Ingenuity program. This program provides information about each gene including reagents related to the gene such

as antibodies, what role it has in apoptosis or growth and diseases. Using this program, an interaction profile is created in order to determine related genes and pathways. Many of the genes that displayed a significantly up- and down-regulated expression were involved in dermatological diseases and conditions such as fibrosis, cell-to-cell signaling, interaction and cellular development. For example, many of the genes that were differentially expressed in the WT and TG mouse keratinocyte RNA were found to be implicated in cardiac fibrosis and cell death (Figure 11), liver fibrosis and proliferation (Figure 12) as well as renal fibrosis and inflammation (Figure 13). This is of intrest to our lab as we study fibrosis and inflammation. Based on gene families and pathways, the ingenuity program linked different genes together, for example MMP-13 and TIMP-2 along with several other genes were linked to dermatological diseases, cell-cell signaling and interaction and cancer. The program also provides a 'Project Summary' that includes the most highly up-regulated and down-regulated genes expressed in the TG compared to the WT mouse keratinocytes (Table 3) based on fold change and p-value. Based on the implications of MMP-13 and its role in wound healing and fibrosis, I chose to focus on MMP-13 and its endogenous inhibitor, TIMP-2. I also looked at CXCL1 and αSMA (also known as ACTA2) due to their expression profiles and their implications in wound healing. The expression profiles for MMP-13, TIMP-2, CXCL1 and αSMA can be seen in Figure 14.

3. 5- Optimizing Primers

Performing a PCR reaction with a temperature gradient at stage 2 optimized the annealing temperatures of the primers. After running the samples on an agarose gel, the strongest signal that corresponded to a certain temperature was chosen as the optimal

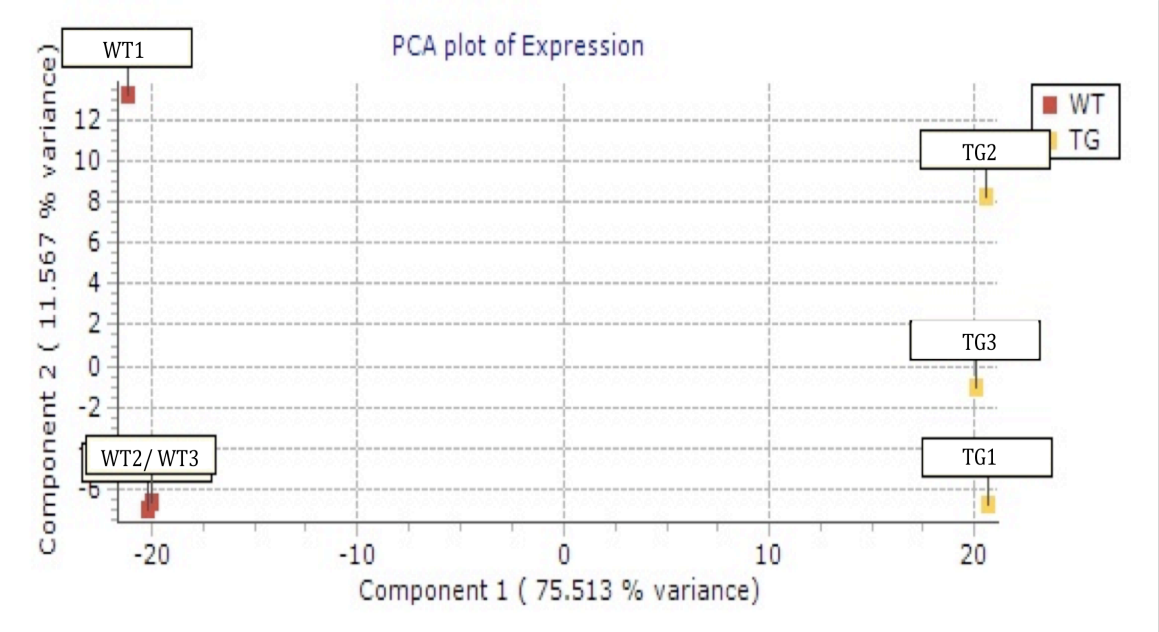

Figure 8: Differential Expression of TG and WT mouse keratinocyte genes. Once the microarray data was collected in the FlexArray program, the genes were plotted on a PCA plot to look at the variance between the TG and WT groups. A variance of 76.513% was found between the groups. This confirmed that there was a significant difference in the gene expression patterns of the TG and WT mouse keratinocytes.

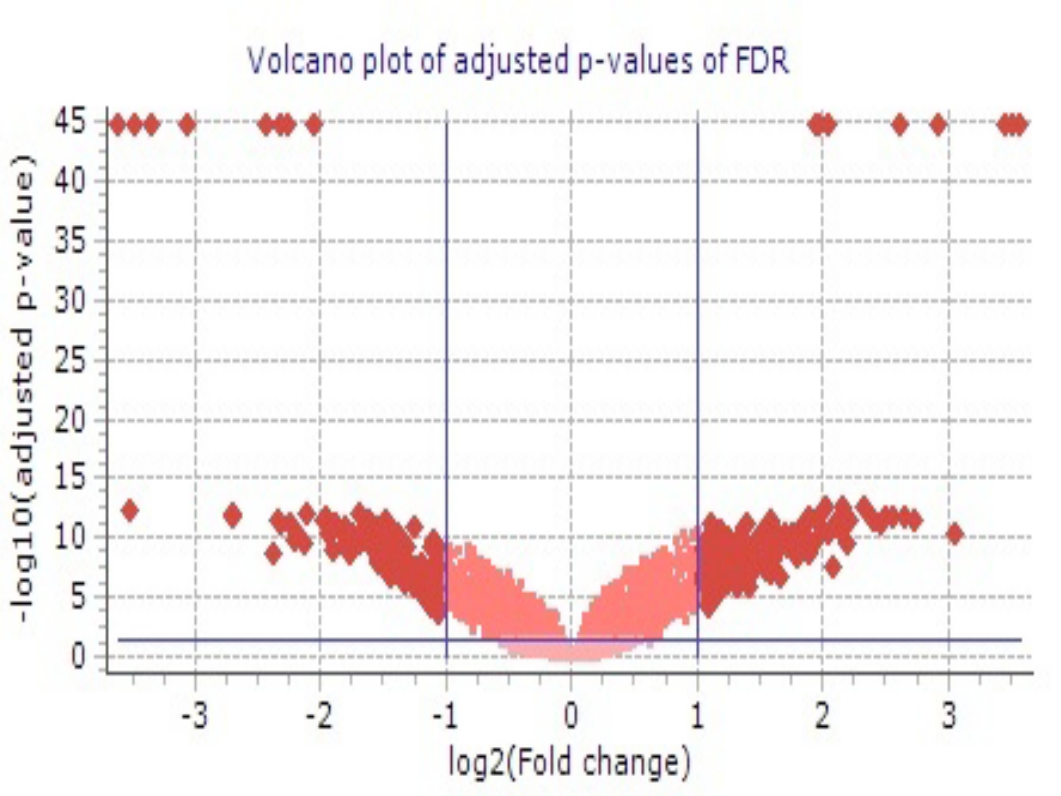

Figure 9: Volcano plot showing genes significantly up-regulated and down-regulated in the TG and WT mouse keratinocytes. Once the statistical analysis was performed using the FlexArray program, the differential expression of genes was analyzed using a volcano plot. The red dots indicate the significantly up- (to the right of +1) and down- (to the left of -1) regulated genes in the TG compared to the WT mouse keratinocytes. The exclusion factor for this study was a fold change between -2 and +2 and a p-value of greater than 0.05. The pink genes did not meet our criteria.

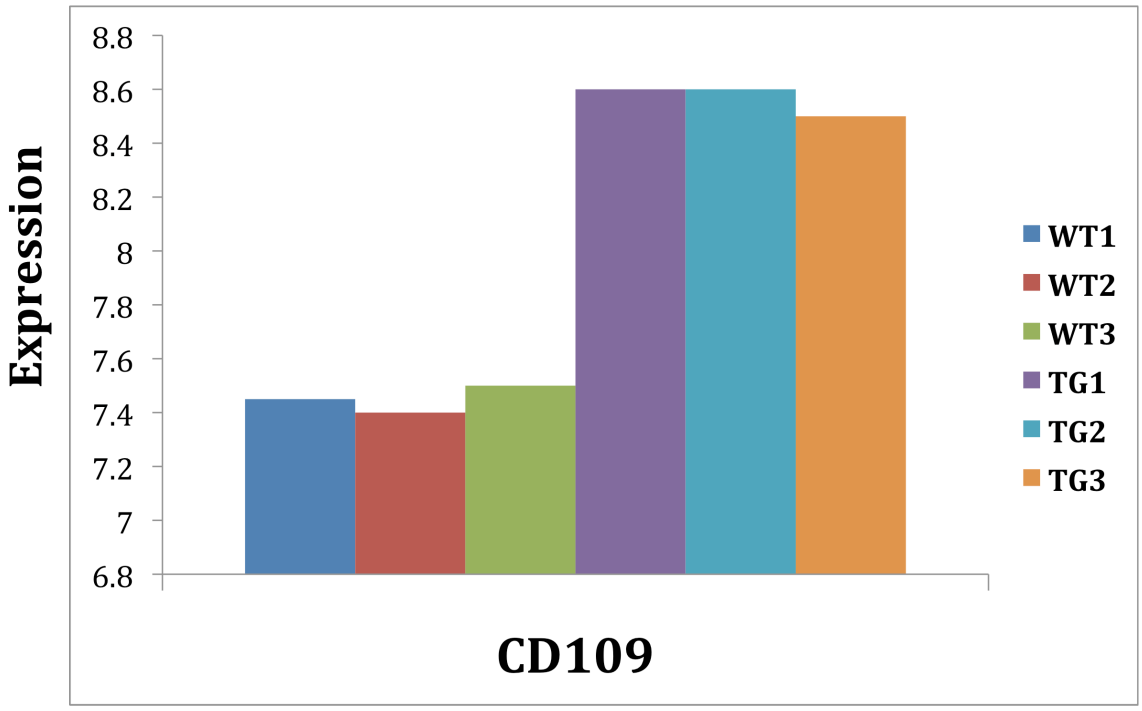

Figure 10: Expression profile of CD109 in TG vs. WT mice. Analysis of the microarray expression profile shows that in all 3 of the keratinocyte samples, CD109 gene expression is increased in the TG keratinocytes compared to their WT counter-parts.

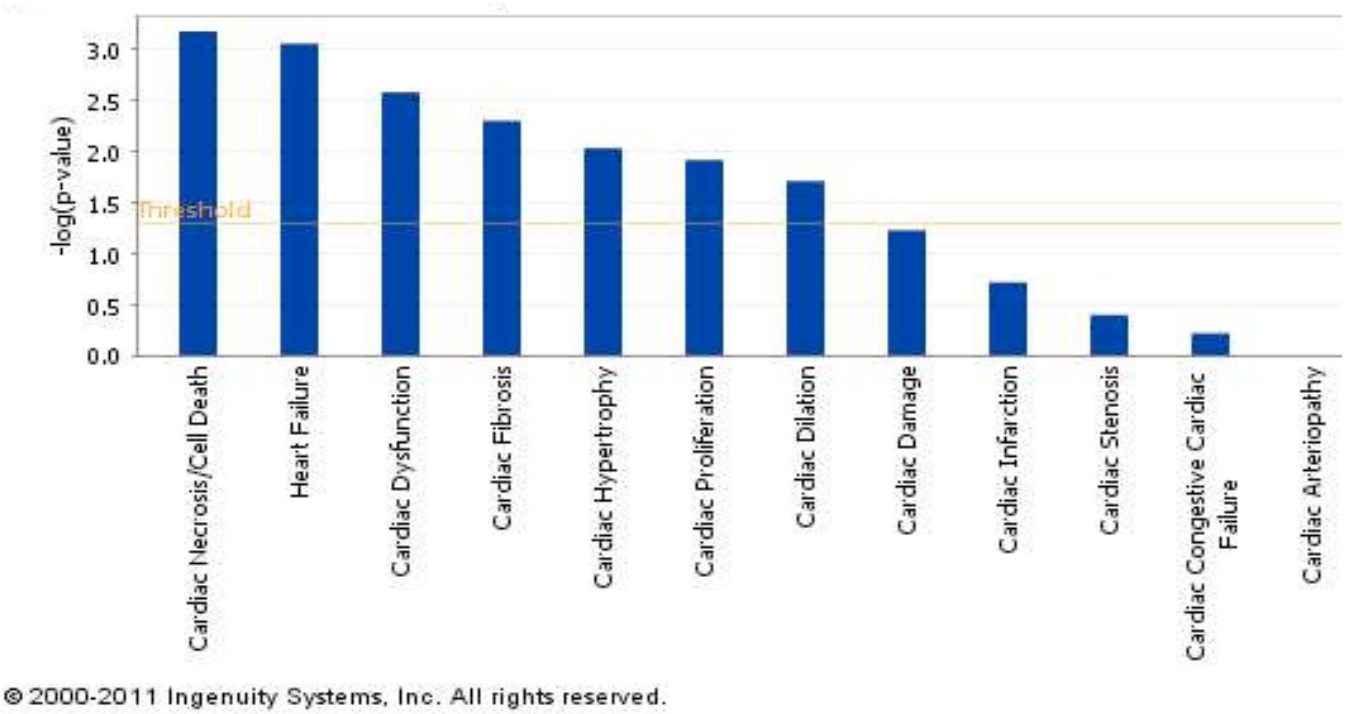

Figure 11. Genes implicated in different cardiac diseases based on –log (p-value). It can be seen that many of the 300 genes differentially expressed in the TG and WT keratinocytes are implicated in cardiac ailments such as necrosis, fibrosis and proliferation.

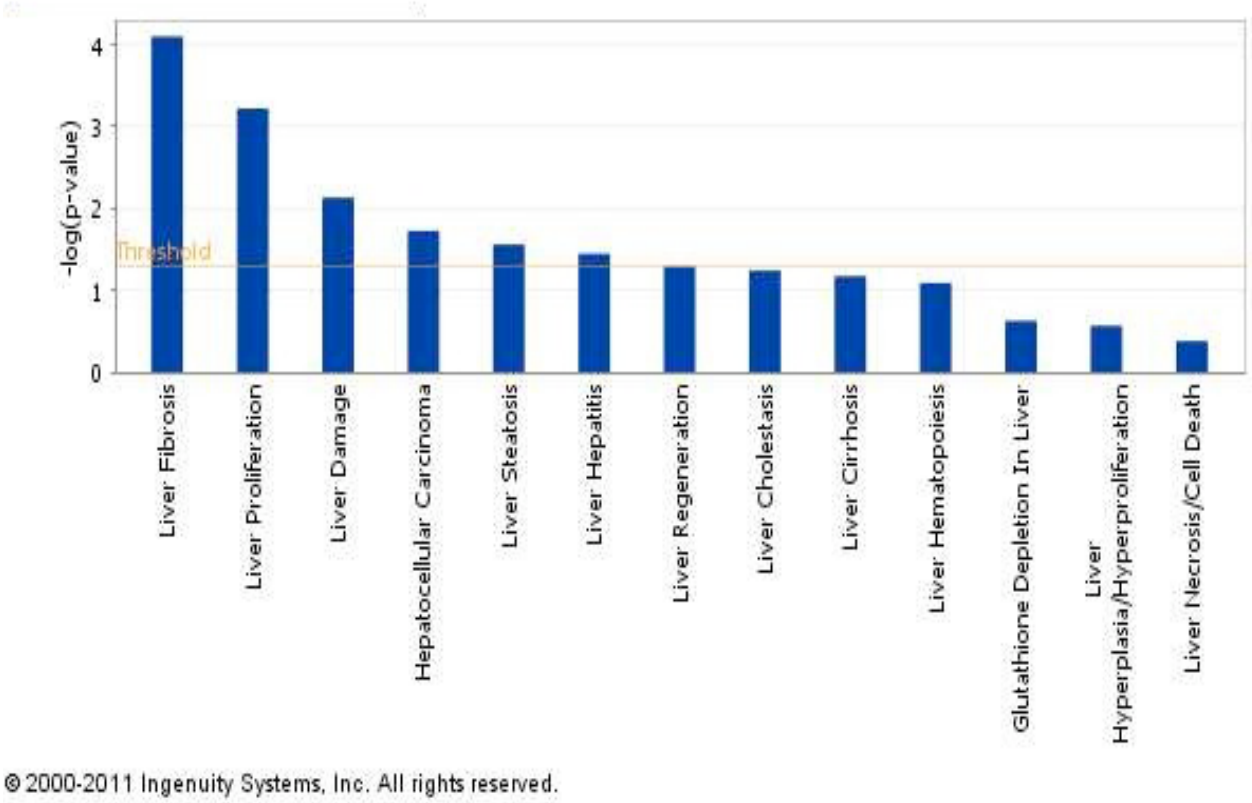

Figure 12. Gene implicated in different liver diseases based on –log (p-value). Many of the 300 genes differentially expressed in the TG and WT keratinocytes are implicated in hepatic ailments such as fibrosis, proliferation and carcinomas.

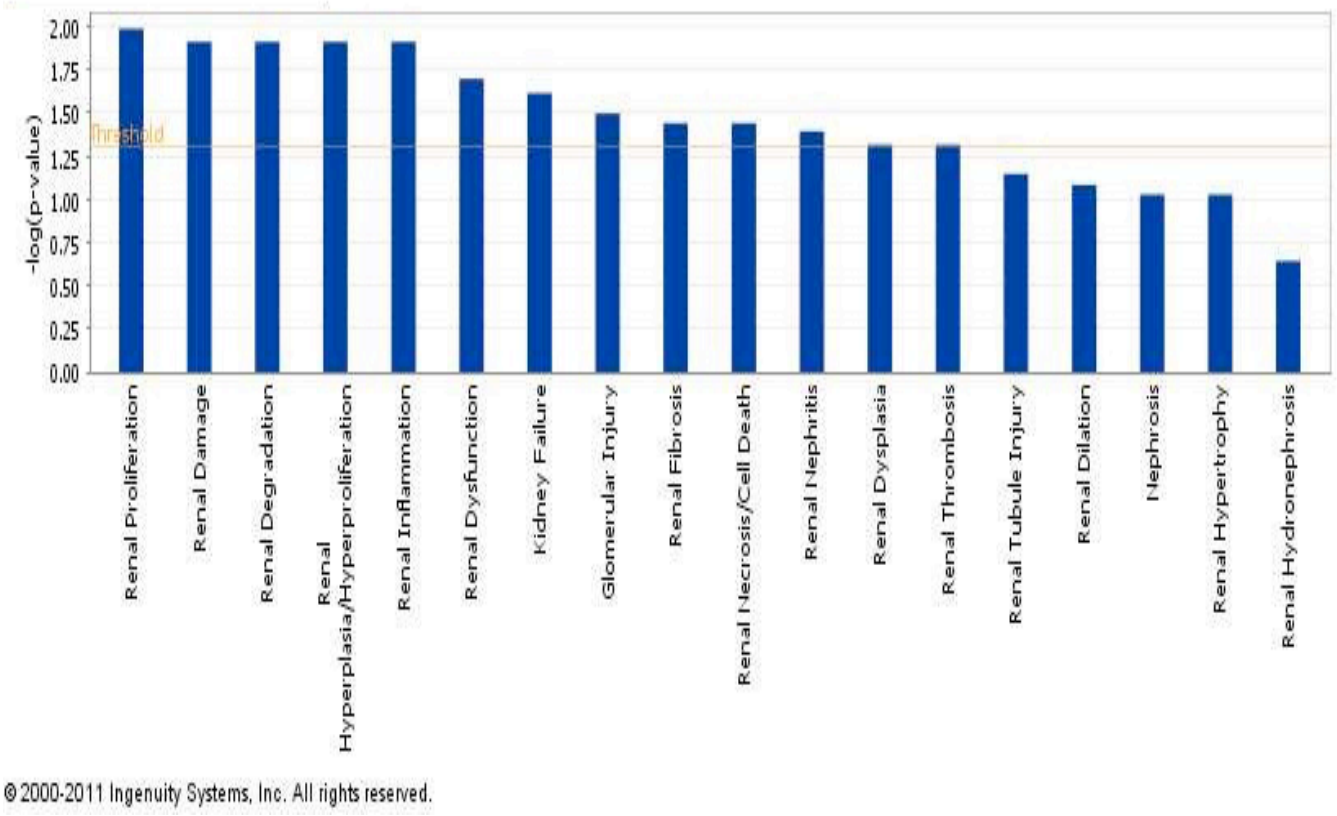

Figure 13. Gene implicated in different renal diseases based on –log (p-value). Many of the 300 genes differentially expressed in the TG and WT keratinocytes are implicated in renal ailments such as fibrosis, proliferation and failure.

a.

Molecule	Expression Value
LPL (Lipoprotein lipase)	↑11.895
CCDC68 (coiled-coil domain containing 68)	↑11.410
MMP13 (matrix metalloproteinase 13)	↑8.366
GPNMB (Transmembrane glycoprotein NMB)	↑6.637
LGALS7 (lectin, galactoside-binding, soluble, 7)	↑6.344
CXCL12 (chemokine (C-X-C motif) ligand 12)	↑6.140
ORM1 (orosomucoid 1)	↑5.891
GUCA2A (guanylate cyclase activator 2A (guanylin))	↑5.716
MGST1 (microsomal glutathione S-transferase 1)	↑5.568
GSTA3 (glutathione S-transferase alpha 3)	↑5.307

b.

Molecule	Expression Value
IL-24 (interleukin 24)	↓-12.181
CXCL1 (chemokine (C-X-C motif) ligand 1)	↓-11.457
ARHGDIB (Rho GDP dissociation inhibitor (GDI) beta)	↓-11.144
SPRR2D (small proline-rich protein 2D)	↓-6.452
GJA1 (gap junction protein, alpha 1)	↓-6.441
FAH (fumarylacetoacetate hydrolase)	↓-5.373
ACTA2 (actin, alpha 2, smooth muscle)	↓-5.157
ALDH2 (aldehyde dehydrogenase 2 family)	↓-5.047
SERPINE2 (erpin peptidase inhibitor, clade E (nexin, plasminogen activator inhibitor type 1), member 2)	↓-4.958
TCEAL8 (transcription elongation factor A (SII)-like 8)	↓-4.801

Table 3: Most highly up- (a) and down- (b) regulated genes in TG compared to WT mouse keratinocytes. The project summary of the Ingenuity program, a list of the 10 most highly up- and down-regulated genes are shown here.

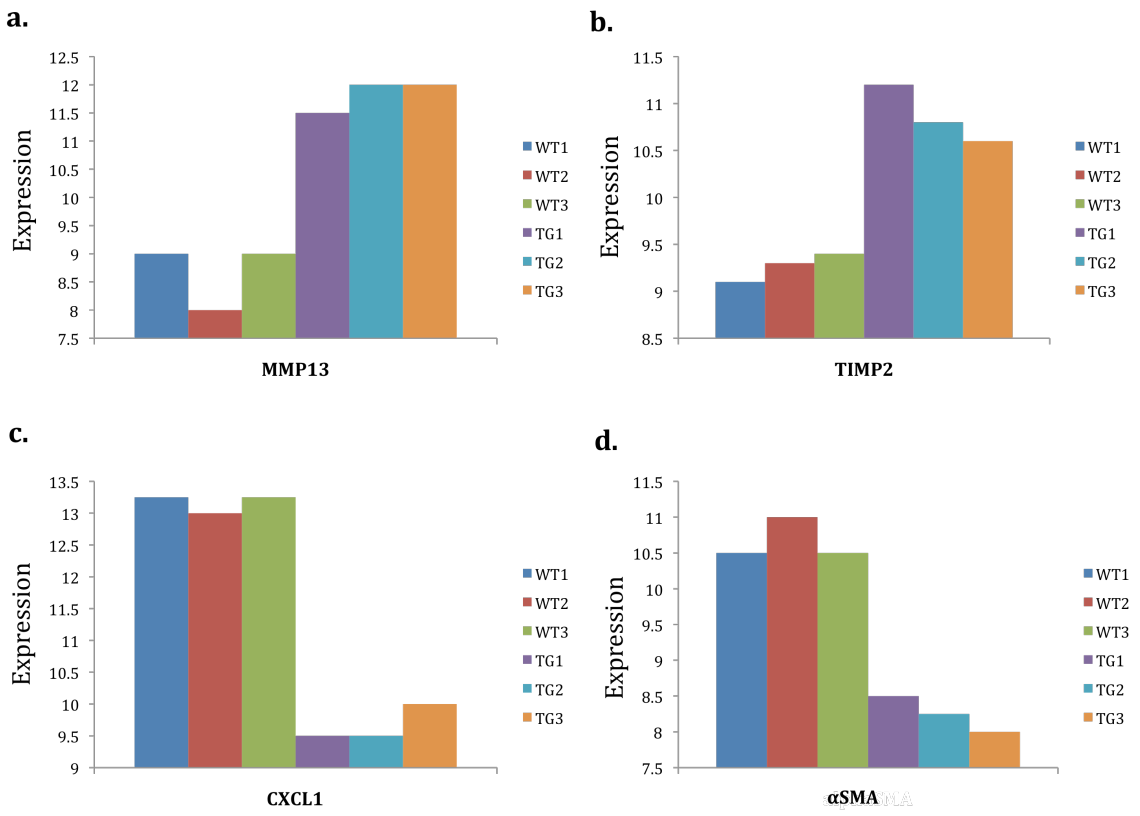

Figure 14: Expression profiles of (a) MMP-13 (b) TIMP-2 (c) CXCL1 and (d) αSMA.

Analysis of the microarray expression profile shows that in all 3 of the keratinocyte samples, MMP-13 and TIMP-2 gene expression is increased in TG compared to WT mouse keratinocytes while the gene expression of CXCL1 and αSMA is decrease in the TG compared to their WT mouse keratinocytes.

annealing temperature of the primer pair. The optimal annealing temperatures for the primers can be seen in Table 4, and were the temperatures used in the semi-quantitative analysis of the cDNA as well as the quantitative analysis done by qRT-PCR.

3.6- Semi-quantitative analysis

Before confirming the microarray array data by running a quantitative RT-PCR, a semi-quantitative PCR was performed. This allowed us to confirm the microarray data in a semi-quantitative manner and confirm the efficacy of the primers. MMP-13 was selected due to its roles in wound healing. Since TIMP-2 is an inhibitor of MMP-13, a gene of interest to this study, it was also selected as one of the up-regulated genes of interest. The microarray results were also validated for CXCL1 and α-SMA because their gene expression in TG compared to WT mouse keratinocytes was found to be highly down-regulated in the summary analysis of the Ingenuity program. MMP-13 gene expression in the TG cDNA samples were found to be highter than that of the WT ones. The same result was seen with TIMP-2. With CXCL1, the expression was lower in the TG when compared to the WT mouse keratinocytes, which confirms the microarray data. αSMA on the other hand showed no difference in expression between the TG and WT mouse keratinocyte cDNA in this semi-quantitative analysis (Figure 15).

3.7- Confirmation of Microarray data

Confirmation of the microarray data is important to validate the results. To confirm the data, a quantitative RT-PCR comparing cDNA prepared from RNA from the TG and WT mouse keratinocytes was done using MMP-13, TIMP-2, CXCL1 and αSMA primers. These

Primer	Annealing Temperature (°C)
CD109	55
GAPDH	55
MMP-13	61
TIMP-2	59
CXCL1	60
αSMA	60
CXCL12	58
IL-24	61

Table 4: Primer annealing temperatures. Optimal primer annealing temperatures were selected after a PCR with a temperature gradient.

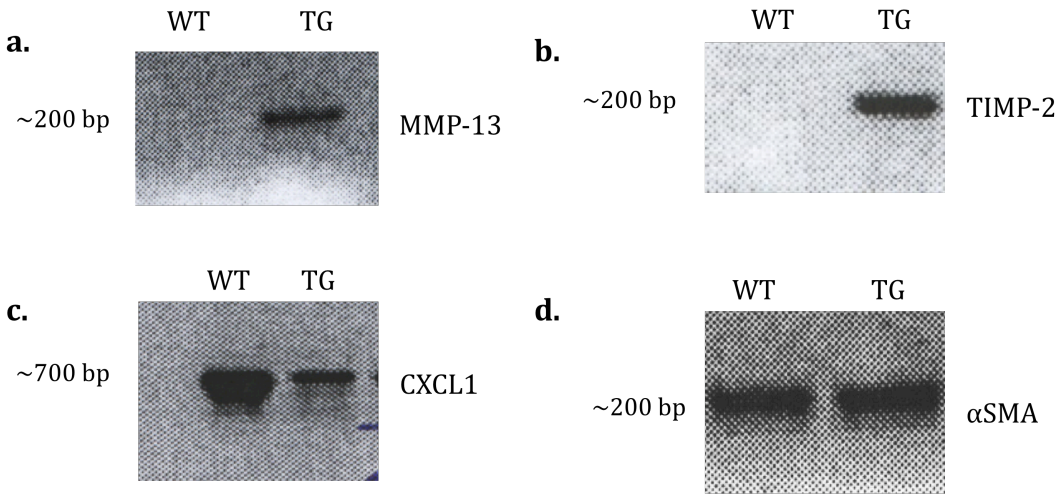

Figure 15: Semi-quantitative analysis of (a) MMP-13, (b) TIMP-2 and (c) CXCL1 (d) αSMA. TG and WT cDNA was run on an agarose gel and the samples were visualized using a UV transilluminator. (a) MMP-13 TG cDNA has a stronger signal than the WT sample; (b) With TIMP-2 the same trend can be seen; (c) A decrease in CXCL1 cDNA can be found in the TG samples in this case; (d) while there seems to be no apparent difference in the expression of αSMA in the TG and WT cDNA. Each experiment was complete 3 times on all 3 WT and TG samples. PCR contamination was ruled out on the basis of a GAPDH gel.

results validate the microarray analysis and furthur confirm that our TG mice exhibit increased expression of MMP-13 (Figure 16a) and TIMP-2 (Figure 16b) and a decreased gene expression of CXCL-1 (Figure 16c) and α-SMA (Figure 16d). Although no difference in αSMA was seen in the gene expression between the TG and WT mouse keratinocytes cDNA in the semi-quantitative analysis, the quantitative RT-PCR analysis confirms what was seen in the microarray (see below).

3.8- Evaluation of MMP-13 expression *in vitro*

The microarray data was obtained using RNA extracted from primary mouse keratinocytes *in vitro*. In order to confirm the up-regulation of MMP-13 at the protein level, a western blot was performed using conditioned media from these cells, as MMP-13 is a secreted protein, whole cell lysates were therefore not used to test MMP-13. For the western blot analysis, a protein assay was done in order to equalize the protein concentrations of all the samples so that the same amount of protein from each sample was loaded in all the lanes of the gel. Also, a picture of the ponceau staining was taken to demonstrate equal protein loading. Figure 17a shows a representative western blot of MMP-13. The results show that the MMP-13 protein is increased in the TG compared to WT mouse keratinocytes although this increase did not achieve statistical significance (Figure 17b).

3.9- Evaluation of MMP-13 expression *in vivo*

Next, I examined if CD109 over-expression regulates the expression of MMP-13 protein *in vivo*. In order evaluate the expression of MMP-13 in the dermis and epidermis;

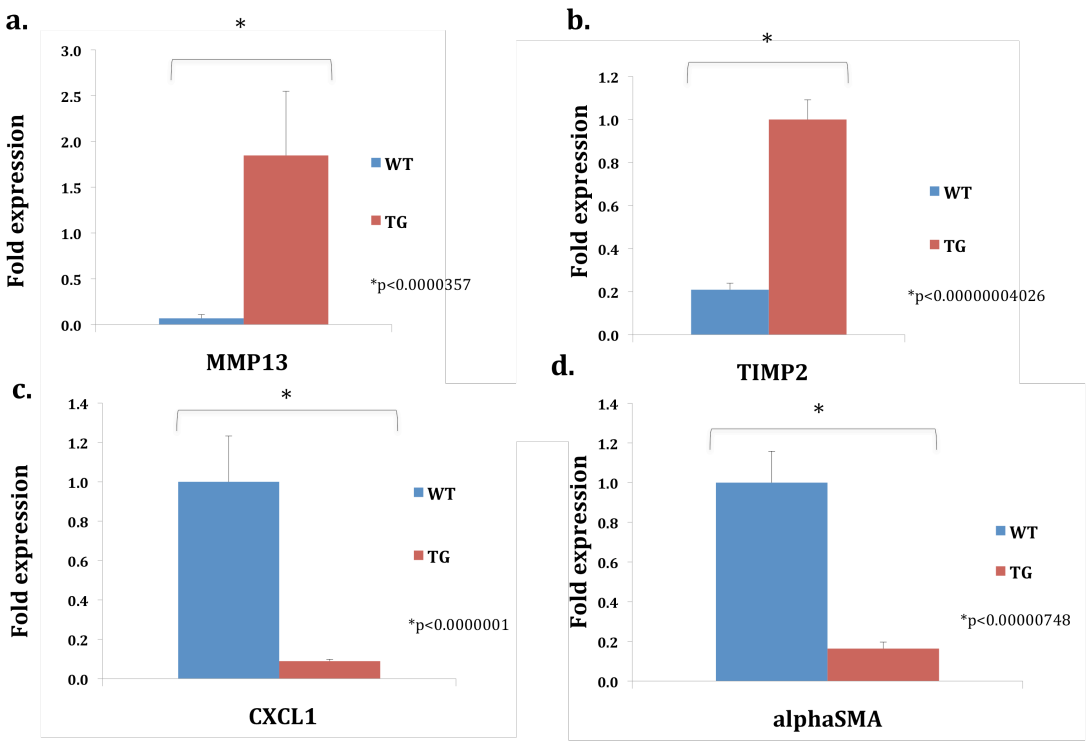

Figure 16: Quantitative analysis of (a) MMP-13, (b) TIMP-2, (c) CXCL1 and (d) αSMA.

The gene expression of MMP-13 and TIMP-2 in the TG mouse keratinocytes compared to the WT is up-regulated and confirms the microarray data. Conversely, the CXCL1 and αSMA gene expression is down-regulated in the TG compared to the WT confirming the microarray data.

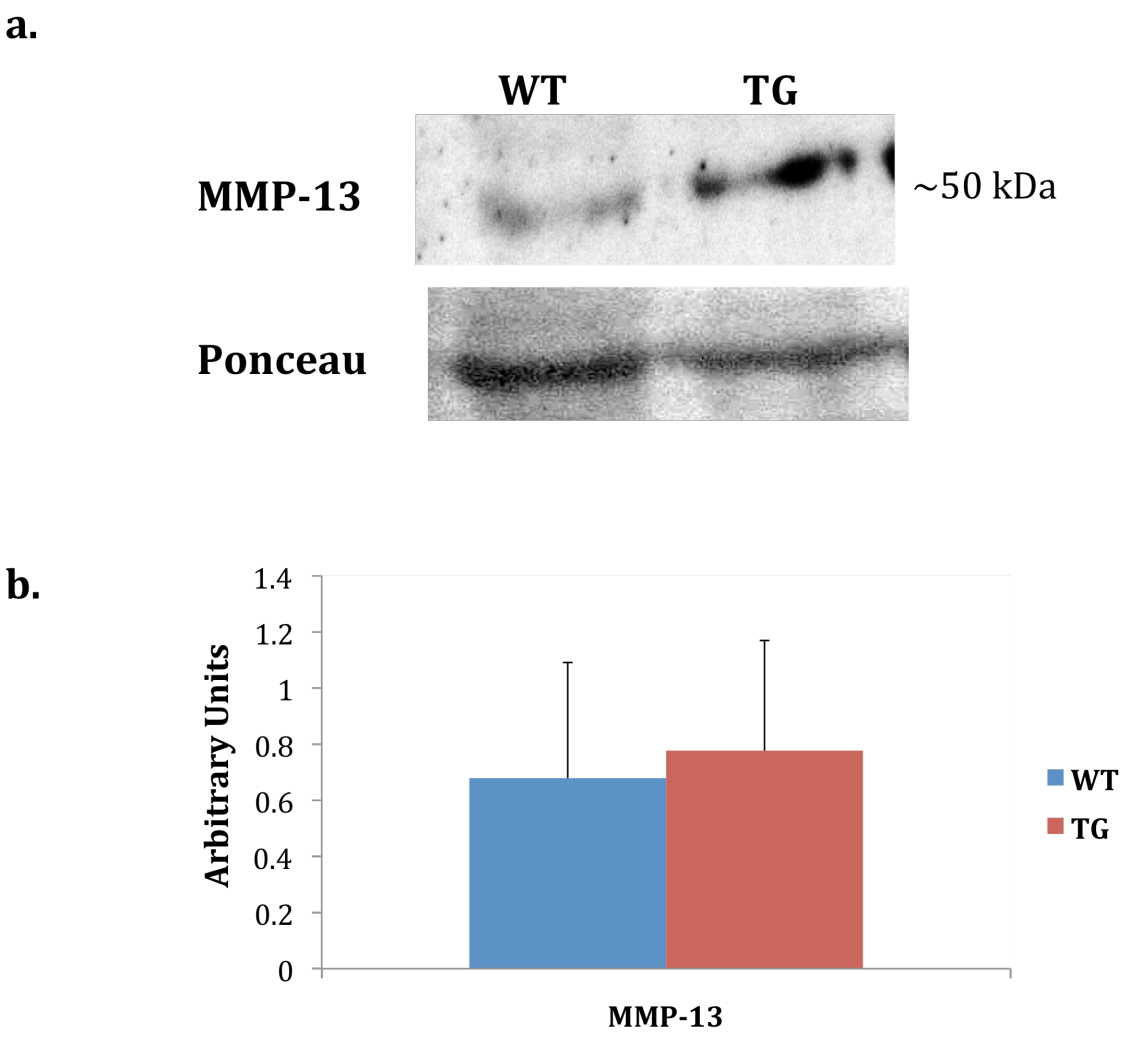

Figure 17: Expression of MMP-13 at the protein level *in vitro.* (a) A western blot analysis showing MMP-13 (~50 kDa) expression. As a loading control, a picture of ponceau is shown. (b) Densitometry analysis demonstrates that there is an increase in MMP-13 protein expression in the TG compared to the WT mouse keratinocyte conditioned media, although this increase was not statistically significant.

immunohistochemistry was performed using an MMP-13 anti-body. Brown staining indicates the presence of MMP-13 in the epidermis and/or dermis. There is more intense brown staining in the TG mice epidermis and dermis indicating that MMP-13 is more highly expressed in TG mice compared to their WT counterparts (Figure 18). This suggests that the TG mice have higher protein levels of MMP-13 which supports results found in our laboratory showing that the TG mice display less scarring upon wounding and better healing parameters.

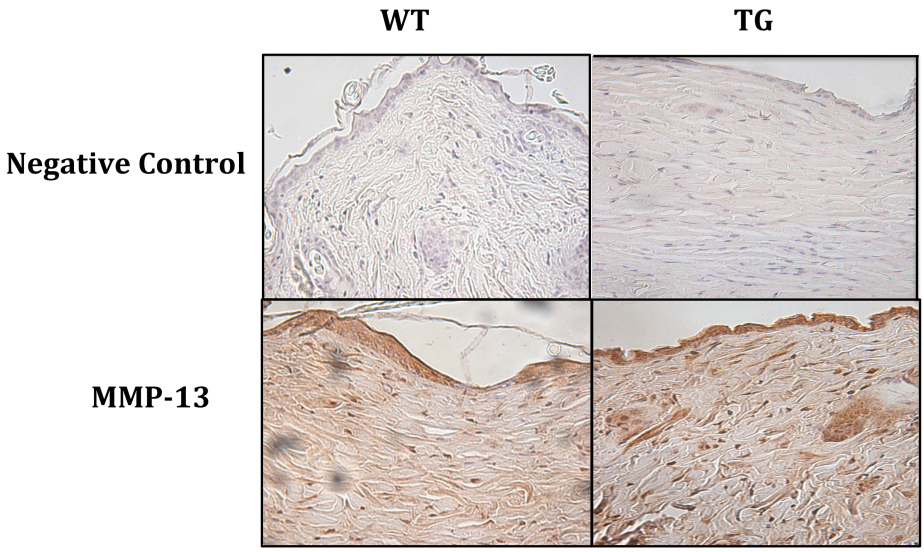

Figure 18: Expression of MMP-13 at the protein level *in vivo* (200x).

Immunohistochemistry for MMP-13 (dilution of antibody 1:500) was performed to detect MMP-13 protein levels *in vivo*. There is more dark brown staining in the TG as compared to the WT mouse tissue, suggesting that more MMP-13 is present in the skin of the TG mice. In the negative control no primary antibody was added to the samples.

CHAPTER 4: DISCUSSION

TGF-β is a multifunctional growth factor that is involved in many aspects of wound healing such as ECM synthesis, cell proliferation, immune responses and angiogenesis (Kane et al 1991, Sellheye et al 1993, Wang et al 1997). TGF-β also drives pro-fibrotic responses by enhancing ECM gene expression and fibroblast proliferation while also repressing catabolic enzymes. At the site of injury, excess TGF-β has been shown to cause hypertrophic scarring (Gerguson and O'Kane 2004), increased dermal thickness and irregular collagen organization leading to impaired wound healing (Cowin et al 2001, Schmid et al 1993).

Our group recently identified CD109 as a novel TGF-β co-receptor, which binds to TβRI and inhibits TGF-β signaling and responses in keratinocytes and fibroblasts (Tam et al 1998). TG mice overexpressing CD109 in the skin, developed in our laboratory, have been used for many *in vitro* and *in vivo* studies showing that CD109 is a potent inhibitor of ECM synthesis (Finnson et al 2006). Our group has previously evaluated the effect of CD109 overexpression in TG mice in both normal excisional wound healing (Vorstebosch et al 2010) and in a bleomycin-induced model of skin fibrosis (Alajmi et al 2010). During excisional wound healing, overexpression of CD109 accelerates wound healing, promotes more rapid resolution of granulation tissue and decreases scarring parameters (Vorstenbosch et al 2010). In the bleomycin-induced skin fibrosis model, characterized by overproduction of ECM in the dermis, TG mice exhibit decreased ECM protein deposition and dermal thickness. Given these promising results, the next step was to determine how the overexpression of CD109 is regulated at the molecular level. The mechanism by which CD109 may exert its effect on wound healing and scarring is not yet well understood. CD109 may regulate the expression of multiple genes important in healing and scarring. A microarray (Illumina) was

performed in order to identify genes that are differentially expressed in TG mouse kerationcytes compared to their WT counterparts.

The microarray was performed at Génome Québec, where RNA samples from TG and WT mouse keratinocytes were analyzed. The mouseWG-6V2 Illumina bead chip was used so that all 6 samples of RNA (3x TG and 3xWT) were analyzed together. Using a whole genome mouse chip allowed us to analyze the difference between the TG and WT mouse keratinocyte gene expression. To evaluate the data from the microarray, the FlexArray program was used for statistical analysis and visualization of microarray expression data. The raw data contained 30,000 genes to be analyzed. Before putting the data through statistical tests, the variance of all the genes in the TG compared to WT samples were evaluated using the PCA plot. This indicated a variation between the two test groups with a percentage different of about 75%. In order to reduce the number of genes to be analyzed, the raw data underwent stringent statistical analysis where the Lumi, Cyber-T and FDR tests were used. From this, a volcano plot was generated for adjusted p-values of FDR. The results show that 168 genes had an increased gene expression in the TG compared to the WT mouse keratinocytes and 132 genes that showed a decrease in gene expression in the TG compared to the WT mouse keratinocytes. The exclusion factor for this was a p-value above 0.05 and a fold change between -2 and +2. The first gene that was examined was CD109, as we know it is overexpressed in the TG mouse keratinocytes. CD109 was found to have a fold increase of 2.17 in the TG compared to WT mouse keratinocytes with a p-value of $9x10^{-15}$.

These 300 genes were put into the Ingenuity program, which helps to analyze the genes by making associations of the genes to specific pathways, diseases and biological functions. Many of these genes were found to be implicated in dermatological diseases,

cancer, cell-to-cell signaling and interactions and fibrosis. This was of interest to us because the research focus of our group is wound healing and dermatological diseases such as scleroderma and fibrosis. After evaluating the list of genes, we found MMP-13 to be highly up-regulated in the TG compared to WT mouse keratinocytes with a fold increase of 8.366 and a p-value of $5.47x10^{-14}$. We also looked for MMP-13 associated genes and found TIMP-2 to be up-regulated in the TG mouse keratinocytes by 3.03 with a p-value of $5.48x\ 10^{-10}$.

MMPs are involved in tissue homeostasis and wound repair (Toriseva and Kahari 2009). They breakdown ECM and are not found in uninjured tissues but are up-regulated during inflammation, repair and remodeling of epithelial cells. In the first stage of wound healing, inflammation, MMPs are expressed by epithelial and stromal cells (Gill and Parks 2008). In the re-epithelialization stage, cell migration is needed so that the dead cells can be discarded and keratinocytes can migrate within the wound. MMPs help in this process by breaking down the ECM and loosening cell-cell and cell-ECM interactions, promoting a shift to tissue repair. In the remodeling stage MMPs start to degrade as collagen is laid down.

In order to validate the microarray results, quantitative RT-PCR was performed on MMP-13 and TIMP-2. qRT-PCR was also performed on highly down-regulated genes, CXCL1 and αSMA, in order to make the validation more robust. We found MMP-13 and TIMP-2 gene expression to be highly up-regulated in the TG cDNA compared to the WT cDNA.

CXCL1 was one of the most highly down-regulated genes in the TG compared to the WT mouse keratinocytes, these results were validated using quantitative RT-PCR. CXCL1 gene expression was decreased in TG compared to the WT mouse keratinocytes. CXCL1 is expressed by macrophages, neutrophils and epithelial cells and is involved in angiogenesis, inflammation, wound healing and tumorigenesis (Zaja-Milatovic and Richmond 2008). MMPs

regulate chemokines by decreasing their expression (Gill and Parks 2008). In the TG mice, we see an increase in the gene expression of MMP-13 and a decrease in the gene expression of CXCL1. MMPs regulate chemokine expression negatively; in this case, the increase in MMP-13 gene expression in the TG mice may cause the decrease in the gene expression of CXCL1.

The fold change in gene expression of αSMA is decreased in TG compared to the WT mouse keratinocytes. α-SMA is important in the contraction of myofibroblasts during wound healing (Hinz et al 2001) and is induced by TGF-β1 (Ronnov-Jessen and Petersen 1993). In this study, TG mouse keratinocytes display a decreased gene expression of α-SMA. Due to TGF-βs actions in promoting α-SMA expression, the decrease in αSMA expression observed in the TG mice support this notion. When CD109 inhibits of the TGF-β signaling pathway, TGF-β can no longer cause an increase in the gene expression of αSMA, leading to its down-regulation. This was seen in the TG mouse keratinocytes which overexpress CD109 as compared to the WT mouse keratinocytes. TGF-βs promotion of αSMA expression is said to contribute to a fibrosis (Hinz et al 2001, Zhang and Phan 1999), this finding may indicate the reason that the TG mice display a decrease in fibrosis.

In order to look at the expression of MMP-13 at the protein level, a western blot was performed on conditioned media for the mouse keratinocytes. The conditioned media was analyzed because MMP-13 is a secreted protein. The results show that the MMP-13 protein is increased in the TG compared to their WT mouse keratinocytes although statistical significance was not reached. As the conditioned media was left on the mouse keratinocytes for only 4 hours, this may be a reason that no significant difference in seen.

In order to determine the expression of MMP-13 *in vivo*, immunohistochemistry was performed. There increased expression of MMP-13 in the TG mice dermis and epidermis

indicating that MMP-13 is more highly expressed in skin of the TG mice when compared to their WT counterparts.

From this study it can be seen that in TG mouse keratinocytes, MMP-13 gene expression is elevated. TGF-β is an inhibitor of MMPs and CD109 is an inhibitor of the TGF-β signaling pathway, which suggests that CD109 may increase the expression of MMPs. In order to determine CD109s direct effect on MMP-13, mechanistic studies of how CD109 regulated MMP-13 expression. Doing *in vitro* studies knocking down CD109 in mouse keratinocytes will help determine if this increase of MMP-13 is due to CD109s direct effect on the TGF-β signaling pathway or if it is an indirect effect. If we decrease the expression of CD109 and see no subsequent increase in MMP-13, like was seen in the TG mouse keratinocytes, then we can infer that the increase gene expression of MMP-13 in the TG mice may be due to the overexpression of CD109.

Upon tissue injury, acute wound healing, MMP expression is elevated and TIMP expression is down-regulated in order to cause ECM degradation to facilitate wound healing. The ECM is degraded so that inflammatory factors can infiltrate the wound bed and begin the wound healing process. During chronic wound healing, MMPs are down-regulated and TIMPs up-regulated (Figure 18). TGF-β plays a critical role in this because it inhibits MMPs but also stimulates TIMP expression. This causes ECM deposition and fibrosis (Knittel et al 1999). Previous studies have shown that CD109 inhibits the TGF-β signaling pathway (Finnson et al 2006). Results shown in the current study indicate that in TG mice MMP-13 gene expression is increased. Although more in depth studies need to be done to confirm CD109s direct effect on MMP-13, it is likely that CD109s inhibitory effect on the TGF-β signaling pathway is

causing the increase in MMP-13 gene expression in the TG compared to their wild-type mouse keratinocytes.

A large number of genes are differentially expressed in the TG keratinocytes overexpressing CD109, compared to their WT counter-parts. MMP-13 and TIMP-2 were shown to have an increase in their gene expression in TG keratinocytes, suggesting that CD109 may modulate wound healing by increasing MMP-13 expression in keratinocytes. In addition to the few genes from the microarray data that I have studied during my master's thesis, there are hundreds of genes, which were differentially expressed in the TG versus the WT mouse keratinocytes. Therefore, the microarray data that I have analyzed has provided a rich source of information for further studies to implicate the role of CD109 in inflammation, fibrosis and wound healing.

APPENDIX

Appendix 1: Up- and down-regulated genes in TG compared to their WT mouse keratinocytes. The probe Id, gene symbol, fold-change in expression and p-value are shown for all 300 genes that were found to be differentially expressed in the TG and WT mouse keratinocytes. This table is in numerical order of fold-change value. For example, the down-regulated genes in the TG mouse keratinocytes have fold-changes between 0.08 and 0.049 whereas the up-regulated genes in the TG mouse keratinocytes have a fold-change between 2.0 and 11.89.

Down-regulated genes in TG mouse keratinocytes compared to WT

Probe Id	Symbol	Fold-change	P-value
6180609	Il24	0.082096	0
3610082	Cxcl1	0.08727962	2.22E-16
1090180	Arhgdib	0.08973128	0
3520053	Ociad2	0.09863742	0
1340446	Gp38	0.1210184	0
6200392	Sprr2d	0.1549846	4.44E-16
1710193	Gja1	0.1552604	8.88E-16
5860348	Fah	0.1861328	0
2140255	Acta2	0.1939129	6.20E-12
2340349	Aldh2	0.1981532	2.44E-15
1850022	Acta2	0.2012497	8.66E-15
870309	Serpine2	0.2016784	0
1070047	Tceal8	0.2082725	0
990438	Cotl1	0.2112064	5.11E-15
1190546	S100a8	0.217104	2.45E-14
430068	Acta2	0.2179983	2.62E-13
5360685	Igfbp7	0.2283803	7.41E-13
6590343	Rab15	0.2314574	5.55E-16
4880433	Upk1b	0.24082	0
2490682	Dpp7	0.2410649	0
3940242	Samd9l	0.2541121	1.89E-15
4480180	Phlda1	0.2605211	1.67E-15

3520546	Emp3	0.2627781	5.34E-14
3850102	Epgn	0.2697401	2.38E-12
730093	Sprr2e	0.2727337	6.33E-15
1690376	Sh3kbp1	0.2739376	8.77E-15
1260482	Sparc	0.2810737	4.27E-14
4040475	Prkg2	0.2843546	3.67E-14
2340131	Igf2bp3	0.287053	4.25E-14
520762	Sh3kbp1	0.2886713	3.51E-14
7100458	2210023G05Rik	0.2892892	1.63E-14
1070097	Hsd17b7	0.2904648	9.32E-13
3130136	Acta2	0.2958353	7.99E-12
3890274	Scd1	0.2990942	7.36E-14
130634	Ddit4	0.2995463	1.55E-13
2470554	Clec2e	0.3124173	4.44E-16
7040181	2410008K03Rik	0.3132501	5.02E-13
6350133	Ociad2	0.3238446	1.21E-14
1170605	Ankk1	0.3262476	1.78E-15
5890487	Gstk1	0.3339619	5.53E-14
2490039	Nrg1	0.3343742	3.07E-13
1070224	Emp3	0.3357747	3.06E-12
5130148	Sparc	0.3387536	1.27E-14
3140328	Ptp4a3	0.343365	1.59E-14
6380059	Ccdc53	0.3440615	1.10E-13
5720180	Alas1	0.3443586	2.51E-11
5690270	Col18a1	0.3447993	7.17E-11
7210072	Irf6	0.3534184	8.12E-11
630025	Mlkl	0.3536503	2.10E-13
240717	Ppard	0.3558582	1.91E-11
7510070	Nme4	0.3563735	3.62E-13
3310537	P4ha2	0.357567	1.12E-12
4570451	Cdkn1c	0.3580616	1.07E-13
6110519	Elk3	0.3596444	8.42E-12
3290523	Gas6	0.3600942	3.77E-15
240259	EG433229	0.36102	1.91E-12
3120703	Cotl1	0.366545	1.88E-13
4880494	Ociad2	0.3668463	5.18E-14
2750326	Egln3	0.3686049	2.10E-14
1990373	Areg	0.3693082	1.32E-09
1500148	Gtse1	0.3695077	1.38E-10
1740167	Clca5	0.3696579	9.25E-14
450553	Lce3b	0.3721527	2.30E-12
4050762	Serpinb2	0.3754823	2.36E-12
1770592	Nuak2	0.3779268	5.11E-12
670253	Rangrf	0.384283	6.25E-14
2850133	Msn	0.3855926	2.15E-11
1090730	Krt6b	0.3873505	5.92E-10
6130561	Plau	0.3884383	2.37E-12

3520221	Lxn	0.3952083	1.22E-11
2490553	Il1a	0.3969377	5.41E-13
4850605	Lamb3	0.3998081	5.45E-09
4480333	Ppic	0.4051878	7.64E-11
3180730	Abhd14b	0.4076597	1.84E-12
60239	Dusp6	0.408004	1.84E-09
3800746	Gm566	0.4082045	2.18E-10
290110	Pfkp	0.4106493	5.54E-11
5700161	Gpr109a	0.412765	2.02E-10
2140402	Dst	0.4155495	1.08E-09
3370487	Ext1	0.4193288	1.83E-10
4610110	Fst	0.4208173	1.08E-08
4070097	Tmem185b	0.4229102	1.63E-14
5890553	Lss	0.42844	4.78E-09
2230538	Cd44	0.4307041	3.78E-09
1400398	2310014H01Rik	0.4336154	7.88E-10
6620079	Egr1	0.439251	4.92E-08
2970392	Krt16	0.4392871	1.29E-08
3130630	Cdkn1a	0.4400339	5.64E-09
1070630	Tnfaip2	0.4406309	8.75E-11
3310243	Mdm2	0.4444048	4.60E-09
2100097	Mvd	0.4522019	2.93E-10
7160349	Nme4	0.4544801	4.45E-10
7560338	Ass1	0.4566151	2.48E-10
4640338	Klf7	0.4571629	9.42E-10
3890332	Gadd45a	0.4594623	4.27E-09
4830674	Itgb6	0.4606758	3.04E-10
7330050	Ptrh1	0.4615488	1.24E-10
3610056	Ppif	0.4623864	4.11E-08
2630647	Prep	0.4631627	1.38E-09
1940445	Dnajc10	0.4631842	5.99E-09
5810039	Lama3	0.4637424	1.60E-06
6520075	Ier3	0.4639423	8.88E-09
4590136	Actn1	0.4640242	1.39E-07
1820091	Lce3b	0.4650185	2.09E-12
6220270	Mcm5	0.4655834	2.02E-09
1410204	Ccng1	0.4656167	4.27E-08
3190669	LOC383897	0.4659322	3.97E-13
130598	Oas1g	0.468493	4.20E-12
4290446	2310007F04Rik	0.4693123	4.80E-11
2450735	Rai14	0.4706035	4.62E-08
60324	Cdsn	0.4722868	5.63E-09
2060382	LOC666559	0.4725657	1.75E-07
2760341	Apaf1	0.4726197	1.06E-10
2000131	Tlr2	0.4744287	9.04E-13
650564	Pgm2	0.4790838	3.20E-08
2320414	Stab1	0.4794312	2.08E-11

2470553	Ptk2	0.479573	6.67E-09
3780619	Tuba1a	0.4796718	1.49E-08
6960441	Cbr3	0.4810106	1.29E-12
6510112	Ybx3	0.4827956	5.17E-06
5260288	Rpl38	0.4847637	3.38E-09
3140274	Dcxr	0.485204	8.13E-08
5690603	Btbd11	0.4854701	9.76E-10
2480551	Aprt	0.4870672	5.70E-08
110661	Acat2	0.488014	4.89E-07
580674	D630040I23Rik	0.4892285	2.40E-10
1780474	Msn	0.4900459	1.02E-10
3290209	Col7a1	0.4932671	6.94E-09
7200270	Chaf1b	0.4943848	3.74E-10
1980603	S100a9	0.4945671	1.37E-11
2140450	1110012O05Rik	0.4956055	3.35E-09
940102	Pscd3	0.496524	1.63E-09

Up-regulated genes in TG mouse keratinocytes compared to WT

Probe Id	Symbol	Fold-change	P-value
5260379	LOC622404	2.001532	1.02E-07
3400646	Sirpa	2.003713	2.07E-09
7610017	Erdr1	2.005253	3.70E-07
6590717	Lsm14b	2.006059	9.56E-09
4040292	Gpnmb	2.009339	2.05E-11
6860291	Mif4gd	2.018061	4.17E-08
3850017	Tgfbr1	2.022881	1.07E-08
6940458	Nudt1	2.024741	1.48E-09
1770181	Spsb2	2.029734	1.25E-11
4560528	Snx2	2.037152	3.73E-08
6660398	Ddrgk1	2.041098	1.63E-08
4570687	Yipf3	2.042333	6.05E-08
1030292	Ints1	2.04393	1.67E-08
7000376	Rdh12	2.062056	1.62E-09
6760397	Edg5	2.066942	5.32E-10
5310091	Add3	2.092745	9.78E-09
4280274	Gdpd1	2.094862	1.50E-08
1340681	Ryk	2.09934	9.52E-10
540475	Slc46a1	2.101011	4.28E-13
2190632	Slc44a2	2.109278	1.21E-08
6770392	Vav3	2.123466	5.50E-10
4280056	Trib3	2.126449	4.98E-09
670133	Hmgn3	2.13522	2.94E-08

1500192	Tjap1	2.138611	3.80E-11
3800706	A030004J04Rik	2.142922	9.64E-10
4670228	Gpnmb	2.143156	1.65E-06
5860521	Figf	2.143919	8.35E-10
540762	Xpa	2.148851	1.16E-10
610707	Krtdap	2.150098	5.09E-11
6180678	Gusb	2.151488	1.41E-09
580364	Igfbp2	2.166265	1.25E-07
3130372	Dctn3	2.166926	4.43E-08
1570594	Socs3	2.168607	6.87E-12
630689	Cd109	2.16929	9.10E-15
3420538	Degs1	2.174071	2.08E-07
3990196	Diras2	2.1748	2.42E-13
5310598	Cryab	2.181535	2.58E-13
5550086	Dusp16	2.185663	3.50E-10
4560228	Cldn3	2.192996	5.24E-12
2850487	Eif1a	2.20967	3.46E-08
6380086	Itpkc	2.209735	3.00E-09
6650349	Micall2	2.210302	9.31E-09
3180068	Akr7a5	2.216307	3.46E-08
6370241	Tpm2	2.22502	1.24E-09
4900360	Tjap1	2.229186	9.07E-11
6130424	Atg12	2.23024	4.45E-09
4480615	Sbsn	2.2391	1.74E-08
3420746	Osbpl9	2.25187	4.16E-08
2690215	Anxa8	2.255312	8.24E-09
1940368	2810432D09Rik	2.256662	2.18E-08
6180348	Crabp2	2.263011	3.97E-11
2570754	Sgpp1	2.285251	2.37E-08
6940762	Atp6v1c2	2.28824	3.91E-14
4250487	Tmem45a	2.289207	2.95E-09
7200021	Sncg	2.301692	1.84E-08
4150739	Cdc42ep3	2.316605	8.94E-10
2190039	Rnase1	2.319467	3.59E-11
4250121	Hmgn3	2.329272	4.46E-09
380102	Ahnak	2.330204	1.25E-09
6650524	Cacna1d	2.344888	1.00E-12
7550360	Tcf4	2.35141	4.09E-12
7210497	Sh3bp5l	2.352692	8.83E-10
3390243	Cpe	2.353689	5.22E-09
3840521	LOC100046232	2.363602	1.34E-10
6380672	Ryk	2.366909	8.01E-09
1450056	Micall2	2.368469	8.80E-11
6280731	Sbsn	2.372824	2.06E-09
5550671	Ly6c1	2.382654	2.51E-10
3400703	Macrod1	2.38582	2.20E-13
3450180	Tmem176b	2.395421	1.30E-10

7330292	Mgst2	2.406227	1.72E-11
6270739	Gcnt2	2.409173	2.51E-11
10730	Cbx6	2.439812	8.02E-11
3800608	Nedd4l	2.443293	3.08E-12
430504	Tmem184a	2.451902	1.21E-10
6350192	2310005L22Rik	2.461992	3.48E-12
5560754	Ly6d	2.47351	1.52E-09
4280131	Slc24a3	2.480866	2.25E-12
540338	Dctn3	2.48314	1.11E-10
2510646	Ly6d	2.487149	2.74E-09
7560639	Cyb5	2.501972	4.02E-09
1230240	Igfbp2	2.503601	9.76E-09
6560093	Sprr1a	2.508248	7.81E-11
7150392	Btbd3	2.546884	1.28E-13
5810327	Btbd3	2.559539	6.95E-13
7650273	Hist1h1c	2.593588	3.89E-12
3370136	Gpc3	2.60799	2.04E-14
3870386	Gm94	2.609077	7.26E-12
5720112	Hoxa7	2.612308	2.78E-10
4040025	Cdh13	2.631956	1.50E-12
1410735	Gpnmb	2.635703	9.74E-13
3710136	2310033F14Rik	2.642233	6.22E-15
3180750	Dbp	2.661785	9.97E-11
6450228	Sprr1b	2.66334	1.77E-08
50079	Hist1h1c	2.688522	1.48E-11
6940367	Ivl	2.716822	6.53E-10
2760333	2310043J07Rik	2.718014	9.15E-10
2480075	Clip4	2.769444	2.02E-11
7050546	Hist2h2aa1	2.814373	5.69E-13
5260482	Wnt4	2.817317	1.85E-13
2630086	9630015D15Rik	2.859628	8.23E-12
3610440	Psap	2.875855	4.97E-11
5560470	Psap	2.881571	1.47E-10
1850685	Eif3b	2.883381	2.24E-11
10768	Gm2a	2.891778	1.28E-12
7400044	Fosl2	2.900761	5.37E-11
7210438	Casp14	2.923922	3.14E-10
6510397	Ankrd47	2.927157	1.53E-14
3890600	Mmp10	2.947263	8.81E-12
6590736	Klk7	2.977309	2.27E-11
6940402	Il15	2.990318	8.56E-12
1850487	Foxq1	2.990428	1.60E-13
2070152	Timp2	3.029389	5.48E-10
630452	Rdhe2	3.030507	2.00E-15
4590129	Ivl	3.059673	4.41E-11
6860309	Nuak1	3.076232	9.24E-12
4730202	2310007B03Rik	3.098673	7.66E-12

5340358	Ccl27	3.13463	5.81E-14
60544	Snx8	3.171468	1.09E-09
620372	Sphk1	3.256265	7.36E-14
1300747	LOC100046120	3.283395	9.10E-14
4900168	Osr2	3.328257	2.03E-12
1660605	Sema5a	3.390334	5.93E-14
1340196	Psapl1	3.399983	9.76E-13
6200446	Klk8	3.444429	1.01E-12
1770324	Wnt4	3.483484	1.88E-11
4070561	Osr2	3.528689	6.91E-14
3800670	Ank	3.576504	1.04E-12
4210327	Klf9	3.592594	1.01E-14
6330672	Dlk2	3.655755	2.44E-15
3130326	Psmg3	3.67329	2.29E-13
2850451	Apcdd1	3.68047	4.55E-15
6130669	Cst3	3.715131	6.18E-12
450356	Acot1	3.727782	1.55E-15
2690435	Peg3	3.878701	0
3170739	Ccl27	3.879776	3.46E-13
3310025	D4Bwg0951e	3.905751	0
1110670	Hist2h2aa2	3.922713	6.11E-15
4890440	Capns2	3.961974	5.55E-16
3850255	Nbl1	4.064199	1.11E-16
7330477	Krt7	4.111155	0
70601	Wfdc2	4.122347	9.39E-14
5260392	Asprv1	4.251711	1.05E-10
2100327	Stard5	4.364211	2.55E-15
1240424	Nupr1	4.393002	2.48E-14
3370397	Barx2	4.457963	1.11E-16
7040184	Lgals7	4.489133	9.99E-16
830333	Krtdap	4.604435	6.14E-13
6020274	Sema5a	4.609328	7.77E-16
2970500	Serpinb6c	4.66511	3.11E-15
270228	Stard5	5.076638	1.11E-16
3780193	Gsta3	5.306592	2.55E-15
7610114	Mgst1	5.56843	7.55E-15
3610554	Guca2a	5.715785	7.77E-16
60196	Orm1	5.890582	7.77E-16
7550112	Cxcl12	6.140176	0
3710520	Lgals7	6.344081	1.33E-15
10193	Gpnmb	6.63704	3.33E-15
5870021	Xlr4a	7.616279	0
5690131	Mmp13	8.366435	5.47E-14
4880524	2310002L13Rik	10.9532	0
4200035	Ccdc68	11.40972	0
5360300	Lpl	11.89541	0

Bibliography

Alajmi, H., Vorstenbosch, J., Winocour, S., Trzeciak., A., Lessard, L., Philip, A. (2010) *Plastic and Reconstructive Surgery.* **125**, 166A.

Annes JP, Munger JS, Rifkin DB (2003). Making sense of latent TGFbeta activation. *J Cell Sci* **116:** 217-224.

Armour A, Scott PG, Tredget EE (2007). Cellular and molecular pathology of HTS: basis for treatment. *Wound Repair Regen* **15 Suppl 1:** S6-17.

Asano Y, Ihn H, Kubo M, Jinnin M, Mimura Y, Ashida R *et al* (2006). Clinical significance of serum matrix metalloproteinase-13 levels in patients with localized scleroderma. *Clin Exp Rheumatol* **24:** 394-399.

Attisano L, Lee-Hoeflich ST (2001). The Smads. *Genome Biol* **2:** REVIEWS3010.

Barrientos S, Stojadinovic O, Golinko MS, Brem H, Tomic-Canic M (2008). Growth factors and cytokines in wound healing. *Wound Repair Regen* **16:** 585-601.

Beck LS, DeGuzman L, Lee WP, Xu Y, Siegel MW, Amento EP (1993). One systemic administration of transforming growth factor-beta 1 reverses age- or glucocorticoid-impaired wound healing. *J Clin Invest* **92:** 2841-2849.

Bennett SP, Griffiths GD, Schor AM, Leese GP, Schor SL (2003). Growth factors in the treatment of diabetic foot ulcers. *Br J Surg* **90:** 133-146.

Blanco FJ, Santibanez JF, Guerrero-Esteo M, Langa C, Vary CP, Bernabeu C (2005). Interaction and functional interplay between endoglin and ALK-1, two components of the endothelial transforming growth factor-beta receptor complex. *J Cell Physiol* **204:** 574-584.

Bobik A (2006). Transforming growth factor-betas and vascular disorders. *Arterioscler Thromb Vasc Biol* **26:** 1712-1720.

Brooks PC, Stromblad S, Sanders LC, von Schalscha TL, Aimes RT, Stetler-Stevenson WG *et al* (1996). Localization of matrix metalloproteinase MMP-2 to the surface of invasive cells by interaction with integrin alpha v beta 3. *Cell* **85:** 683-693.

Chapnick DA, Liu X (2010). Analysis of ligand-dependent nuclear accumulation of Smads in TGF-beta signaling. *Methods Mol Biol* **647:** 95-111.

Cheifetz S, Andres JL, Massague J (1988). The transforming growth factor-beta receptor type III is a membrane proteoglycan. Domain structure of the receptor. *J Biol Chem* **263:** 16984-16991.

Cheifetz S, Hernandez H, Laiho M, ten Dijke P, Iwata KK, Massague J (1990). Distinct transforming growth factor-beta (TGF-beta) receptor subsets as determinants of cellular responsiveness to three TGF-beta isoforms. *J Biol Chem* **265:** 20533-20538.

Cheifetz S, Bellon T, Cales C, Vera S, Bernabeu C, Massague J *et al* (1992). Endoglin is a component of the transforming growth factor-beta receptor system in human endothelial cells. *J Biol Chem* **267:** 19027-19030.

Chen Y, Shi-Wen X, van Beek J, Kennedy L, McLeod M, Renzoni EA *et al* (2005). Matrix contraction by dermal fibroblasts requires transforming growth factor-beta/activin-linked kinase 5, heparan sulfate-containing proteoglycans, and MEK/ERK: insights into pathological scarring in chronic fibrotic disease. *Am J Pathol* **167:** 1699-1711.

Cordeiro MF, Reichel MB, Gay JA, D'Esposita F, Alexander RA, Khaw PT (1999). Transforming growth factor-beta1, -beta2, and -beta3 in vivo: effects on normal and mitomycin C-modulated conjunctival scarring. *Invest Ophthalmol Vis Sci* **40:** 1975-1982.

Cowin AJ, Hatzirodos N, Holding CA, Dunaiski V, Harries RH, Rayner TE *et al* (2001). Effect of healing on the expression of transforming growth factor beta(s) and their receptors in chronic venous leg ulcers. *J Invest Dermatol* **117:** 1282-1289.

D'Angelo M, Billings PC, Pacifici M, Leboy PS, Kirsch T (2001). Authentic matrix vesicles contain active metalloproteases (MMP). a role for matrix vesicle-associated MMP-13 in activation of transforming growth factor-beta. *J Biol Chem* **276:** 11347-11353.

de Caestecker MP, Yahata T, Wang D, Parks WT, Huang SX, Hill CS *et al* (2000). The Smad4 activation domain (SAD) is a proline-rich, p300-dependent transcriptional activation domain. *Journal of Biological Chemistry* **275:** 2115-2122.

Desmouliere A, Chaponnier C, Gabbiani G (2005). Tissue repair, contraction, and the myofibroblast. *Wound Repair Regen* **13:** 7-12.

Dickson MC, Martin JS, Cousins FM, Kulkarni AB, Karlsson S, Akhurst RJ (1995). Defective haematopoiesis and vasculogenesis in transforming growth factor-beta 1 knock out mice. *Development* **121:** 1845-1854.

Ebisawa T, Fukuchi M, Murakami G, Chiba T, Tanaka K, Imamura T *et al* (2001). Smurf1 interacts with transforming growth factor-beta type I receptor through Smad7 and induces receptor degradation. *J Biol Chem* **276:** 12477-12480.

Eickelberg O, Centrella M, Reiss M, Kashgarian M, Wells RG (2002). Betaglycan inhibits TGF-beta signaling by preventing type I-type II receptor complex formation. Glycosaminoglycan modifications alter betaglycan function. *J Biol Chem* **277:** 823-829.

Feng XH, Derynck R (2005). Specificity and versatility in tgf-beta signaling through Smads. *Annu Rev Cell Dev Biol* **21:** 659-693.

Ferguson MW, O'Kane S (2004). Scar-free healing: from embryonic mechanisms to adult therapeutic intervention. *Philos Trans R Soc Lond B Biol Sci* **359:** 839-850.

Finnson KW, Tam BY, Liu K, Marcoux A, Lepage P, Roy S *et al* (2006). Identification of CD109 as part of the TGF-beta receptor system in human keratinocytes. *Faseb J* **20:** 1525-1527.

Finnson KW, Parker WL, ten Dijke P, Thorikay M, Philip A (2008). ALK1 opposes ALK5/Smad3 signaling and expression of extracellular matrix components in human chondrocytes. *J Bone Miner Res* **23:** 896-906.

Finnson KW, Parker WL, Chi Y, Hoemann CD, Goldring MB, Antoniou J *et al* (2010). Endoglin differentially regulates TGF-beta-induced Smad2/3 and Smad1/5 signalling and its expression correlates with extracellular matrix production and cellular differentiation state in human chondrocytes. *Osteoarthritis Cartilage* **18:** 1518-1527.

Flechsig P, Hartenstein B, Teurich S, Dadrich M, Hauser K, Abdollahi A *et al* (2010). Loss of matrix metalloproteinase-13 attenuates murine radiation-induced pulmonary fibrosis. *Int J Radiat Oncol Biol Phys* **77:** 582-590.

Fukushima D, Butzow R, Hildebrand A, Ruoslahti E (1993). Localization of transforming growth factor beta binding site in betaglycan. Comparison with small extracellular matrix proteoglycans. *J Biol Chem* **268:** 22710-22715.

Gailit J, Welch MP, Clark RA (1994). TGF-beta 1 stimulates expression of keratinocyte integrins during re-epithelialization of cutaneous wounds. *J Invest Dermatol* **103:** 221-227.

Gill SE, Parks WC (2008). Metalloproteinases and their inhibitors: regulators of wound healing. *Int J Biochem Cell Biol* **40:** 1334-1347.

Gordon KJ, Blobe GC (2008). Role of transforming growth factor-beta superfamily signaling pathways in human disease. *Biochim Biophys Acta* **1782:** 197-228.

Goumans MJ, Valdimarsdottir G, Itoh S, Rosendahl A, Sideras P, ten Dijke P (2002). Balancing the activation state of the endothelium via two distinct TGF-beta type I receptors. *Embo J* **21:** 1743-1753.

Goumans MJ, Lebrin F, Valdimarsdottir G (2003). Controlling the angiogenic switch: a balance between two distinct TGF-b receptor signaling pathways. *Trends Cardiovasc Med* **13:** 301-307.

Gray AM, Mason AJ (1990). Requirement for activin A and transforming growth factor--beta 1 pro-regions in homodimer assembly. *Science* **247:** 1328-1330.

Graycar JL, Miller DA, Arrick BA, Lyons RM, Moses HL, Derynck R (1989). Human transforming growth factor-beta 3: recombinant expression, purification, and biological

activities in comparison with transforming growth factors-beta 1 and -beta 2. *Mol Endocrinol* **3:** 1977-1986.

Grinnell F, Zhu M, Parks WC (1998). Collagenase-1 complexes with alpha2-macroglobulin in the acute and chronic wound environments. *J Invest Dermatol* **110:** 771-776.

Guo S, Dipietro LA (2010). Factors affecting wound healing. *J Dent Res* **89:** 219-229.

Guo X, Wang XF (2009). Signaling cross-talk between TGF-beta/BMP and other pathways. *Cell Res* **19:** 71-88.

Gurtner GC, Werner S, Barrandon Y, Longaker MT (2008). Wound repair and regeneration. *Nature* **453:** 314-321.

Hagiwara S, Murakumo Y, Sato T, Shigetomi T, Mitsudo K, Tohnai I *et al* (2008). Up-regulation of CD109 expression is associated with carcinogenesis of the squamous epithelium of the oral cavity. *Cancer Sci* **99:** 1916-1923.

Hagiwara S, Murakumo Y, Mii S, Shigetomi T, Yamamoto N, Furue H *et al* (2010). Processing of CD109 by furin and its role in the regulation of TGF-beta signaling. *Oncogene* **29:** 2181-2191.

Haregewoin A, Solomon K, Hom RC, Soman G, Bergelson JM, Bhan AK *et al* (1994). Cellular expression of a GPI-linked T cell activation protein. *Cell Immunol* **156:** 357-370.

Hartenstein B, Dittrich BT, Stickens D, Heyer B, Vu TH, Teurich S *et al* (2006). Epidermal development and wound healing in matrix metalloproteinase 13-deficient mice. *J Invest Dermatol* **126:** 486-496.

Hashimoto M, Ichihara M, Watanabe T, Kawai K, Koshikawa K, Yuasa N *et al* (2004). Expression of CD109 in human cancer. *Oncogene* **23:** 3716-3720.

Hata A, Lagna G, Massague J, Hemmati-Brivanlou A (1998). Smad6 inhibits BMP/Smad1 signaling by specifically competing with the Smad4 tumor suppressor. *Genes Dev* **12:** 186-197.

Hattori N, Mochizuki S, Kishi K, Nakajima T, Takaishi H, D'Armiento J *et al* (2009). MMP-13 plays a role in keratinocyte migration, angiogenesis, and contraction in mouse skin wound healing. *Am J Pathol* **175:** 533-546.

Hayashi H, Abdollah S, Qiu Y, Cai J, Xu YY, Grinnell BW *et al* (1997). The MAD-related protein Smad7 associates with the TGFbeta receptor and functions as an antagonist of TGFbeta signaling. *Cell* **89:** 1165-1173.

Henis YI, Moustakas A, Lin HY, Lodish HF (1994). The types II and III transforming growth factor-beta receptors form homo-oligomers. *J Cell Biol* **126:** 139-154.

Hill CS (2009). Nucleocytoplasmic shuttling of Smad proteins. *Cell Res* **19:** 36-46.

Hinz B, Celetta G, Tomasek JJ, Gabbiani G, Chaponnier C (2001). Alpha-smooth muscle actin expression upregulates fibroblast contractile activity. *Mol Biol Cell* **12:** 2730-2741.

Huse M, Muir TW, Xu L, Chen YG, Kuriyan J, Massague J (2001). The TGF beta receptor activation process: an inhibitor- to substrate-binding switch. *Mol Cell* **8:** 671-682.

Hussein MR (2005). Transforming growth factor-beta and malignant melanoma: molecular mechanisms. *J Cutan Pathol* **32:** 389-395.

Hyytiainen M, Penttinen C, Keski-Oja J (2004). Latent TGF-beta binding proteins: extracellular matrix association and roles in TGF-beta activation. *Crit Rev Clin Lab Sci* **41:** 233-264.

Imamura T, Takase M, Nishihara A, Oeda E, Hanai J, Kawabata M *et al* (1997). Smad6 inhibits signalling by the TGF-beta superfamily. *Nature* **389:** 622-626.

Javelaud D, Alexaki VI, Mauviel A (2008). Transforming growth factor-beta in cutaneous melanoma. *Pigment Cell Melanoma Res* **21:** 123-132.

Jenkins G (2008). The role of proteases in transforming growth factor-beta activation. *Int J Biochem Cell Biol* **40:** 1068-1078.

Jude EB, Blakytny R, Bulmer J, Boulton AJ, Ferguson MW (2002). Transforming growth factor-beta 1, 2, 3 and receptor type I and II in diabetic foot ulcers. *Diabet Med* **19:** 440-447.

Kane CJ, Hebda PA, Mansbridge JN, Hanawalt PC (1991). Direct evidence for spatial and temporal regulation of transforming growth factor beta 1 expression during cutaneous wound healing. *J Cell Physiol* **148:** 157-173.

Kantola AK, Keski-Oja J, Koli K (2008). Fibronectin and heparin binding domains of latent TGF-beta binding protein (LTBP)-4 mediate matrix targeting and cell adhesion. *Exp Cell Res* **314:** 2488-2500.

Kavsak P, Rasmussen RK, Causing CG, Bonni S, Zhu H, Thomsen GH *et al* (2000). Smad7 binds to Smurf2 to form an E3 ubiquitin ligase that targets the TGF beta receptor for degradation. *Mol Cell* **6:** 1365-1375.

Kirkbride KC, Ray BN, Blobe GC (2005). Cell-surface co-receptors: emerging roles in signaling and human disease. *Trends Biochem Sci* **30:** 611-621.

Klass BR, Grobbelaar AO, Rolfe KJ (2009). Transforming growth factor beta1 signalling, wound healing and repair: a multifunctional cytokine with clinical implications for wound repair, a delicate balance. *Postgrad Med J* **85:** 9-14.

Knittel T, Mehde M, Kobold D, Saile B, Dinter C, Ramadori G (1999). Expression patterns of matrix metalloproteinases and their inhibitors in parenchymal and non-parenchymal cells of rat liver: regulation by TNF-alpha and TGF-beta1. *J Hepatol* **30:** 48-60.

Koch RM, Roche NS, Parks WT, Ashcroft GS, Letterio JJ, Roberts AB (2000). Incisional wound healing in transforming growth factor-beta1 null mice. *Wound Repair Regen* **8:** 179-191.

Koli K, Wempe F, Sterner-Kock A, Kantola A, Komor M, Hofmann WK *et al* (2004). Disruption of LTBP-4 function reduces TGF-beta activation and enhances BMP-4 signaling in the lung. *J Cell Biol* **167:** 123-133.

Krishna M, Narang H (2008). The complexity of mitogen-activated protein kinases (MAPKs) made simple. *Cell Mol Life Sci* **65:** 3525-3544.

Kurisaki A, Kurisaki K, Kowanetz M, Sugino H, Yoneda Y, Heldin CH *et al* (2006). The mechanism of nuclear export of Smad3 involves exportin 4 and Ran. *Mol Cell Biol* **26:** 1318-1332.

Lamar JM, Iyer V, DiPersio CM (2008). Integrin alpha3beta1 potentiates TGFbeta-mediated induction of MMP-9 in immortalized keratinocytes. *J Invest Dermatol* **128:** 575-586.

Leask A, Abraham DJ (2004). TGF-beta signaling and the fibrotic response. *Faseb J* **18:** 816-827.

Lebrin F, Goumans MJ, Jonker L, Carvalho RL, Valdimarsdottir G, Thorikay M *et al* (2004). Endoglin promotes endothelial cell proliferation and TGF-beta/ALK1 signal transduction. *Embo J* **23:** 4018-4028.

Letamendia A, Lastres P, Botella LM, Raab U, Langa C, Velasco B *et al* (1998). Role of endoglin in cellular responses to transforming growth factor-beta. A comparative study with betaglycan. *J Biol Chem* **273:** 33011-33019.

Li AG, Wang D, Feng XH, Wang XJ (2004). Latent TGFbeta1 overexpression in keratinocytes results in a severe psoriasis-like skin disorder. *Embo J* **23:** 1770-1781.

Li AG, Lu SL, Han G, Kulesz-Martin M, Wang XJ (2005). Current view of the role of transforming growth factor beta 1 in skin carcinogenesis. *J Investig Dermatol Symp Proc* **10:** 110-117.

Li AG, Lu SL, Han G, Hoot KE, Wang XJ (2006). Role of TGFbeta in skin inflammation and carcinogenesis. *Mol Carcinog* **45:** 389-396.

Liu C, Xu P, Lamouille S, Xu J, Derynck R (2009). TACE-mediated ectodomain shedding of the type I TGF-beta receptor downregulates TGF-beta signaling. *Mol Cell* **35:** 26-36.

Lopez-Casillas F, Wrana JL, Massague J (1993). Betaglycan presents ligand to the TGF beta signaling receptor. *Cell* **73:** 1435-1444.

Lopez-Casillas F, Payne HM, Andres JL, Massague J (1994). Betaglycan can act as a dual modulator of TGF-beta access to signaling receptors: mapping of ligand binding and GAG attachment sites. *J Cell Biol* **124:** 557-568.

Madlener M (1998). Differential expression of matrix metalloproteinases and their physiological inhibitors in acute murine skin wounds. *Arch Dermatol Res* **290 Suppl:** S24-29.

Margadant C, Sonnenberg A (2010). Integrin-TGF-beta crosstalk in fibrosis, cancer and wound healing. *EMBO Rep* **11:** 97-105.

Massague J (1998). TGF-beta signal transduction. *Annu Rev Biochem* **67:** 753-791.

Massague J, Seoane J, Wotton D (2005). Smad transcription factors. *Genes Dev* **19:** 2783-2810.

Massague J (2008). TGFbeta in Cancer. *Cell* **134:** 215-230.

Moali C, Hulmes DJ (2009). Extracellular and cell surface proteases in wound healing: new players are still emerging. *Eur J Dermatol* **19:** 552-564.

Montesano R, Orci L (1988). Transforming growth factor beta stimulates collagen-matrix contraction by fibroblasts: implications for wound healing. *Proc Natl Acad Sci U S A* **85:** 4894-4897.

Mu D, Cambier S, Fjellbirkeland L, Baron JL, Munger JS, Kawakatsu H *et al* (2002). The integrin alpha(v)beta8 mediates epithelial homeostasis through MT1-MMP-dependent activation of TGF-beta1. *J Cell Biol* **157:** 493-507.

Mulder G (2004). Electroporatic delivery of TGF-beta1 gene works synergistically with electric therapy to enhance diabetic wound healing in db/db mice. *J Invest Dermatol* **123:** xi.

Murphy-Ullrich JE, Poczatek M (2000). Activation of latent TGF-beta by thrombospondin-1: mechanisms and physiology. *Cytokine Growth Factor Rev* **11:** 59-69.

Mythreye K, Blobe GC (2009). Proteoglycan signaling co-receptors: roles in cell adhesion, migration and invasion. *Cell Signal* **21:** 1548-1558.

Nagarajan RP, Zhang J, Li W, Chen Y (1999). Regulation of Smad7 promoter by direct association with Smad3 and Smad4. *J Biol Chem* **274:** 33412-33418.

Nagase H, Visse R, Murphy G (2006). Structure and function of matrix metalloproteinases and TIMPs. *Cardiovasc Res* **69:** 562-573.

Nakao A, Afrakhte M, Moren A, Nakayama T, Christian JL, Heuchel R *et al* (1997). Identification of Smad7, a TGFbeta-inducible antagonist of TGF-beta signalling. *Nature* **389:** 631-635.

O'Kane S, Ferguson MW (1997). Transforming growth factor beta s and wound healing. *Int J Biochem Cell Biol* **29:** 63-78.

Ohta M, Greenberger JS, Anklesaria P, Bassols A, Massague J (1987). Two forms of transforming growth factor-beta distinguished by multipotential haematopoietic progenitor cells. *Nature* **329:** 539-541.

Olofsson A, Ichijo H, Moren A, ten Dijke P, Miyazono K, Heldin CH (1995). Efficient association of an amino-terminally extended form of human latent transforming growth factor-beta binding protein with the extracellular matrix. *J Biol Chem* **270:** 31294-31297.

Ozdamar B, Bose R, Barrios-Rodiles M, Wang HR, Zhang Y, Wrana JL (2005). Regulation of the polarity protein Par6 by TGFbeta receptors controls epithelial cell plasticity. *Science* **307:** 1603-1609.

Parker WL, Goldring MB, Philip A (2003). Endoglin is expressed on human chondrocytes and forms a heteromeric complex with betaglycan in a ligand and type II TGFbeta receptor independent manner. *J Bone Miner Res* **18:** 289-302.

Proetzel G, Pawlowski SA, Wiles MV, Yin M, Boivin GP, Howles PN *et al* (1995). Transforming growth factor-beta 3 is required for secondary palate fusion. *Nat Genet* **11:** 409-414.

Ronnov-Jessen L, Petersen OW (1993). Induction of alpha-smooth muscle actin by transforming growth factor-beta 1 in quiescent human breast gland fibroblasts. Implications for myofibroblast generation in breast neoplasia. *Lab Invest* **68:** 696-707.

Saharinen J, Keski-Oja J (2000). Specific sequence motif of 8-Cys repeats of TGF-beta binding proteins, LTBPs, creates a hydrophobic interaction surface for binding of small latent TGF-beta. *Mol Biol Cell* **11:** 2691-2704.

Saika S, Ikeda K, Yamanaka O, Miyamoto T, Ohnishi Y, Sato M *et al* (2005). Expression of Smad7 in mouse eyes accelerates healing of corneal tissue after exposure to alkali. *Am J Pathol* **166:** 1405-1418.

Sanford LP, Ormsby I, Gittenberger-de Groot AC, Sariola H, Friedman R, Boivin GP *et al* (1997). TGFbeta2 knockout mice have multiple developmental defects that are non-overlapping with other TGFbeta knockout phenotypes. *Development* **124:** 2659-2670.

Sato T, Murakumo Y, Hagiwara S, Jijiwa M, Suzuki C, Yatabe Y *et al* (2007). High-level expression of CD109 is frequently detected in lung squamous cell carcinomas. *Pathol Int* **57:** 719-724.

Schiller M, Javelaud D, Mauviel A (2004). TGF-beta-induced SMAD signaling and gene regulation: consequences for extracellular matrix remodeling and wound healing. *J Dermatol Sci* **35:** 83-92.

Schmid P, Cox D, Bilbe G, McMaster G, Morrison C, Stahelin H *et al* (1993). TGF-beta s and TGF-beta type II receptor in human epidermis: differential expression in acute and chronic skin wounds. *J Pathol* **171:** 191-197.

Segarini PR, Rosen DM, Seyedin SM (1989). Binding of transforming growth factor-beta to cell surface proteins varies with cell type. *Mol Endocrinol* **3:** 261-272.

Seifert O, Mrowietz U (2009). Keloid scarring: bench and bedside. *Arch Dermatol Res* **301:** 259-272.

Sellheyer K, Bickenbach JR, Rothnagel JA, Bundman D, Longley MA, Krieg T *et al* (1993). Inhibition of skin development by overexpression of transforming growth factor beta 1 in the epidermis of transgenic mice. *Proc Natl Acad Sci U S A* **90:** 5237-5241.

Shah M, Foreman DM, Ferguson MW (1995). Neutralisation of TGF-beta 1 and TGF-beta 2 or exogenous addition of TGF-beta 3 to cutaneous rat wounds reduces scarring. *J Cell Sci* **108 (Pt 3):** 985-1002.

Shi Y, Massague J (2003). Mechanisms of TGF-beta signaling from cell membrane to the nucleus. *Cell* **113:** 685-700.

Shull MM, Ormsby I, Kier AB, Pawlowski S, Diebold RJ, Yin M *et al* (1992). Targeted disruption of the mouse transforming growth factor-beta 1 gene results in multifocal inflammatory disease. *Nature* **359:** 693-699.

Singer AJ, Clark RA (1999). Cutaneous wound healing. *N Engl J Med* **341:** 738-746.

Sirard C, de la Pompa JL, Elia A, Itie A, Mirtsos C, Cheung A *et al* (1998). The tumor suppressor gene Smad4/Dpc4 is required for gastrulation and later for anterior development of the mouse embryo. *Genes Dev* **12:** 107-119.

Sjoblom T, Jones S, Wood LD, Parsons DW, Lin J, Barber TD *et al* (2006). The consensus coding sequences of human breast and colorectal cancers. *Science* **314:** 268-274.

Souchelnytskyi S, ten Dijke P, Miyazono K, Heldin CH (1996). Phosphorylation of Ser165 in TGF-beta type I receptor modulates TGF-beta1-induced cellular responses. *Embo J* **15:** 6231-6240.

Stopa M, Anhuf D, Terstegen L, Gatsios P, Gressner AM, Dooley S (2000). Participation of Smad2, Smad3, and Smad4 in transforming growth factor beta (TGF-beta)-induced activation of Smad7. THE TGF-beta response element of the promoter requires functional Smad binding element and E-box sequences for transcriptional regulation. *J Biol Chem* **275:** 29308-29317.

Sutherland DR, Yeo E, Ryan A, Mills GB, Bailey D, Baker MA (1991). Identification of a cell-surface antigen associated with activated T lymphoblasts and activated platelets. *Blood* **77:** 84-93.

Tam BY, Germain L, Philip A (1998). TGF-beta receptor expression on human keratinocytes: a 150 kDa GPI-anchored TGF-beta1 binding protein forms a heteromeric complex with type I and type II receptors. *J Cell Biochem* **70:** 573-586.

Tam BY, Larouche D, Germain L, Hooper NM, Philip A (2001). Characterization of a 150 kDa accessory receptor for TGF-beta 1 on keratinocytes: direct evidence for a GPI anchor and ligand binding of the released form. *J Cell Biochem* **83:** 494-507.

Tam BY, Finnson KW, Philip A (2003). Glycosylphosphatidylinositol-anchored proteins regulate transforming growth factor-beta signaling in human keratinocytes. *J Biol Chem* **278:** 49610-49617.

Toriseva M, Kahari VM (2009). Proteinases in cutaneous wound healing. *Cell Mol Life Sci* **66:** 203-224.

Tredget EB, Demare J, Chandran G, Tredget EE, Yang L, Ghahary A (2005). Transforming growth factor-beta and its effect on reepithelialization of partial-thickness ear wounds in transgenic mice. *Wound Repair Regen* **13:** 61-67.

Tsukazaki T, Chiang TA, Davison AF, Attisano L, Wrana JL (1998). SARA, a FYVE domain protein that recruits Smad2 to the TGFbeta receptor. *Cell* **95:** 779-791.

Tyrone JW, Marcus JR, Bonomo SR, Mogford JE, Xia Y, Mustoe TA (2000). Transforming growth factor beta3 promotes fascial wound healing in a new animal model. *Arch Surg* **135:** 1154-1159.

Verrecchia F, Vindevoghel L, Lechleider RJ, Uitto J, Roberts AB, Mauviel A (2001). Smad3/AP-1 interactions control transcriptional responses to TGF-beta in a promoter-specific manner. *Oncogene* **20:** 3332-3340.

Vorstenbosch, J., Gallant-Behm, C., Trzeciak, A., Fang, R., Mustoe, T., Philip, A. (2010) Overexpression of CD109 in the epidermis reduces inflammation, improves wound healing and scarring. *Plastic and Reconstructive Surgery.* 125, 98A.

Wang G, Long J, Matsuura I, He D, Liu F (2005). The Smad3 linker region contains a transcriptional activation domain. *Biochem J* **386:** 29-34.

Wang XJ, Greenhalgh DA, Bickenbach JR, Jiang A, Bundman DS, Krieg T *et al* (1997). Expression of a dominant-negative type II transforming growth factor beta (TGF-beta) receptor in the epidermis of transgenic mice blocks TGF-beta-mediated growth inhibition. *Proc Natl Acad Sci U S A* **94:** 2386-2391.

Weinstein M, Yang X, Li C, Xu X, Gotay J, Deng CX (1998). Failure of egg cylinder elongation and mesoderm induction in mouse embryos lacking the tumor suppressor smad2. *Proc Natl Acad Sci U S A* **95:** 9378-9383.

White RA, Malkoski SP, Wang XJ (2010). TGFbeta signaling in head and neck squamous cell carcinoma. *Oncogene* **29:** 5437-5446.

Wieser R, Wrana JL, Massague J (1995). GS domain mutations that constitutively activate T beta R-I, the downstream signaling component in the TGF-beta receptor complex. *Embo J* **14:** 2199-2208.

Wong SH, Hamel L, Chevalier S, Philip A (2000). Endoglin expression on human microvascular endothelial cells association with betaglycan and formation of higher order complexes with TGF-beta signalling receptors. *Eur J Biochem* **267:** 5550-5560.

Wrana JL, Attisano L, Carcamo J, Zentella A, Doody J, Laiho M *et al* (1992). TGF beta signals through a heteromeric protein kinase receptor complex. *Cell* **71:** 1003-1014.

Wrana JL, Attisano L, Wieser R, Ventura F, Massague J (1994). Mechanism of activation of the TGF-beta receptor. *Nature* **370:** 341-347.

Wu JW, Krawitz AR, Chai J, Li W, Zhang F, Luo K *et al* (2002). Structural mechanism of Smad4 recognition by the nuclear oncoprotein Ski: insights on Ski-mediated repression of TGF-beta signaling. *Cell* **111:** 357-367.

Yang L, Chan T, Demare J, Iwashina T, Ghahary A, Scott PG *et al* (2001). Healing of burn wounds in transgenic mice overexpressing transforming growth factor-beta 1 in the epidermis. *Am J Pathol* **159:** 2147-2157.

Yi JY, Shin I, Arteaga CL (2005). Type I transforming growth factor beta receptor binds to and activates phosphatidylinositol 3-kinase. *J Biol Chem* **280:** 10870-10876.

Zaja-Milatovic S, Richmond A (2008). CXC chemokines and their receptors: A case for a significant biological role in cutaneous wound healing. *Histol Histopathol* **23:** 1399-1407.

Zhang HY, Phan SH (1999). Inhibition of myofibroblast apoptosis by transforming growth factor beta(1). *Am J Respir Cell Mol Biol* **21:** 658-665.

Zhang JM, Hashimoto M, Kawai K, Murakumo Y, Sato T, Ichihara M *et al* (2005). CD109 expression in squamous cell carcinoma of the uterine cervix. *Pathol Int* **55:** 165-169.

Zhang S, Fei T, Zhang L, Zhang R, Chen F, Ning Y *et al* (2007). Smad7 antagonizes transforming growth factor beta signaling in the nucleus by interfering with functional Smad-DNA complex formation. *Mol Cell Biol* **27:** 4488-4499.

Zhang W, Jiang Y, Wang Q, Ma X, Xiao Z, Zuo W *et al* (2009). Single-molecule imaging reveals transforming growth factor-beta-induced type II receptor dimerization. *Proc Natl Acad Sci U S A* **106:** 15679-15683.